REPORT DOCUMENTATION PAGE

Form Approved
OMB No. 074-0188

1. AGENCY USE ONLY (Leave blank)	2. REPORT DATE	3. REPORT TYPE AND DATES COVERED
	1995	Technical Report, July 25, 1995

4. TITLE AND SUBTITLE
Forward to Creation of System of Underwater Monitoring of Marine Mammals (SUMMM) in the Eastern Arctic

5. FUNDING NUMBERS
Subcontract PO No. 31-960002-01-94

6. AUTHOR(S)
Dr. Vladimir Baronkin, Dr. Valery Kodanev

7. PERFORMING ORGANIZATION NAME(S) AND ADDRESS(ES)
N.N. Andreyev Acoustics Institute
Moscow, Russia

8. PERFORMING ORGANIZATION REPORT NUMBER
N/A

9. SPONSORING / MONITORING AGENCY NAME(S) AND ADDRESS(ES)
SERDP
901 North Stuart St. Suite 303
Arlington, VA 22203

10. SPONSORING / MONITORING AGENCY REPORT NUMBER
N/A

11. SUPPLEMENTARY NOTES
Report for Science Application International Corporation, Volume II.

12a. DISTRIBUTION / AVAILABILITY STATEMENT
Approved for public release: distribution is unlimited

12b. DISTRIBUTION CODE
A

13. ABSTRACT ***(Maximum 200 Words)***

In the second volume of the report the first results related to creation of hardware and software for the acoustical system of marine mammals (MM) monitoring (MM) are presented. The main object of the system (further SUMMM - System of Underwater Monitoring of Marine Mammals - is used as the abbreviation for such as system) consists in the analysis of adverse influence of human activity on MM. Although suggested methods of SUMMM creation can be used for wide spectrum of situations. Here the main emphasis is made on the adverse influence of powerful low-frequency sound radiation in connection with the realization of ATOC (Acoustic Thermometry of Ocean Climate) project in the Eastern Arctic.

14. SUBJECT TERMS
SERDP, ATOC, SUMMM, MM

15. NUMBER OF PAGES
108

16. PRICE CODE
N/A

17. SECURITY CLASSIFICATION OF REPORT	18. SECURITY CLASSIFICATION OF THIS PAGE	19. SECURITY CLASSIFICATION OF ABSTRACT	20. LIMITATION OF ABSTRACT
unclass	unclass	unclass	UL

N.N. Andreyev Acoustics Institute

FORWARD TO CREATION OF SYSTEM OF UNDERWATER MONITORING OF MARINE MAMMALS (SUMMM) IN THE EASTERN ARCTIC

Report for Science Applications International Corporation

Volume 2

Subcontract

PO N o 31-960002-01-94

Principal Investigators:

Dr. Vladimir Baronkin

Dr. Valery Kodanev

APPROVED

Director AAI, Professor

N .A. Dubrovsky

Moscow 1995

The list of the authors

V.Baronkin (introduction, chapter 1, section 3.1, 3.2, conclusion, proposal)

V.Kodanev (section 2.1, 3.2, 4.1)

Y.Tutekin (section 2.2, chapter 4, section 5.2)

Y.Tuzhilkin (section 2.3, 2.4)

M.Ermolaev (section 2.3)

L.Mokrinskaya (section 5.2).

CONTENTS

INTRODUCTION.

In the second volume of the report the first results related to creation of hardware and software for the acoustical system of marine mammals (MM) monitoring (MM) are presented. The main object of the system (further SUMMM - System of Underwater Monitoring of Marine Mammals - is used as the abreviation for such a system) consists in the analysis of adverse influence of human activity on MM. Although suggested methods of SUMMM creation can be used for wide spectrum of situations. Here main emphasis is made on the adverse influence of powerful low-frequency sound radiation in connection with the realization of ATOC (Acoustic Thermometry of Ocean Climate) project in the Eastern Arctic.

A primary objective of the investigation at given preliminary stage had been development of general principles of the SUMMM construction. It should be noted that the SUMMM creation is complicated scientific and engineering problem though.

Other objective has been in the organization of investigations related to creation of the program package for design of the SUMMM at various environment conditions and the choice of specific structure of the SUMMM under settings up of the SUMMM at the place of statement (the choice of an array configuration, spatial-time signal processing algorithms and so on). This program package (SUMMM-PAC) operates in interactive regime with user and allows the SUMMM efficiency to be evaluated. The SUMMM-PAC includes the database of the MM signals, the database of the statistical characteristics of noise which is characteristic for chosen regions of the ocean, the database of sound propagation conditions for corresponding regions of the ocean and etc. In given stage of the project we have developed the first version of SUMMM-PAC with corresponding software. If allows to incorporate in the SUMMM-PAC new data concerning MM signals, ocean noise, propagation conditions and various methods of sound field calculation, field processing algorithms, variants of SUMMM efficiency

evaluation.

The main goal of the acoustical monitoring of MM is presented in the first volume of the report. Here the possible ways of the SUMMM construction based on the principles of passive and active location are discussed also.

In the second chapter the possible models of signals radiated by an acoustic source from tagged MM are presented. Here the MM signals are briefly described also. In the second chapter the data concerning sound propagation in given region of Eastern Arctic and corresponding noise characteristics are presented as well as.

The preliminary analysis of two chosen two variants of SUMMM is given in the third chapter. The first variant uses the artificial signals from tagged MM, whereas the second variant - the own signals of MM. In addition, for first variant the possibility of transmission of telemetric information with respect to main physiological parameters of MM (pulse rate, respiration rate, diving duration and etc) is considered.

The forth chapter deals with the description of first version of the SUMMM-PAC for the evaluation of the SUMMM efficiency when relatively simple efficiency criteria (detection zones and general ambiguity function) are used.

The results of efficiency calculation for some variants of the SUMMM are given in the fifth chapter. Here the SUMMM with the use of telemetric system are investigated. For the SUMMM using the MM signals directly the SUMMM efficiency is calculated when the matched field processing algorithms are applied. In doing this, the loss in SUMMM efficiency under "mismatching" is estimated also.

The brief calculation and our consideration with respect to future investigations for the project realization completes the report.

I. OBJECTIVES AND METHODS OF THE MONITORING. THE POSSIBLE WAYS OF THE SUMMM CONSTRUCTION.

The marine mammals (MM) is an important part of the nature and have ardent need for protection from an adverse human activity. In particularly, this is true for the adverse influence of the low-frequency powerful sound radiation under implementation of ocean tomography (for example, ATOC project), geophysical research and etc [1]. In our case the acoustical system of monitoring climate of the Eastern Arctic is implied. The emitter of this system have been spaced north of Franz Josef Land.

One effective way of the determination of above mentioned adverse human activity is the organization of continuous surveillance system for tracking of behavior of individual MM and group of MM. At short distances it is possible the use a telemetric system for the tracking of some physiological parameters line pulse rate, respiration rate, brain potentials and so on of the tagged mammals.

These surveillance systems can be based on principles both of passive and of active location. Due to these systems the following main problems of the monitoring of MM can be solved:

- detection of an individual MM and a group of MM;
- localization of an individual MM and a group of MM;
- tracking an individual MM and a group of MM in 3D space and the estimation of parameters of their movement;
- identification of an individual MM and a group of MM, including approximate estimation of a number of MM in the group.

The creation of above mentioned systems is a complicated scientific and engineering problem. Especially it is true under the solution of MM identification problem.

Let us list the following main problem to be solved: the development of appropriate models of MM signals and signals of group of MM, the analysis of sound propagation conditions in chosen region of the ocean (where the system is placed) and the development of corresponding models for possible use of matched field processing when the system is operated at long distances; the measurement of noise statistical characteristics in the chosen region and the construction of an appropriate model of noise; the development of spatial-time processing algorithms for detection, localization, tracking and identification; the choice of type of signals and methods of radiation, when the signals from tagged MM are used.

The SUMMM must be constructed step-by-step. At first the simple systems are constructed and their experimental testing is produced. Furthermore, the development of more complicated and effective system is completed using the obtained experimental results. However, all long we must tend to rational compromise between the simplicity of SUMMM implementation and its efficiency.

Under the use of passive SUMMM two variants are possible: the localization of the acoustic source of tagged MM and the localization of the own MM signals .

The operation range for first variant the SUMMM is largely determined by the power of an acoustic source and the chosen band of frequency. These characteristics must be chosen for reason of MM safety. For example, the sensitivity of pennipeds to sounds with the frequencies in the band 60 ÷ 70 KHz is tens decibels less than in the band 30 ÷ 40 KHz. The above mentioned constraints together with constraints connected with the restrictions on the service life of power cell give rise to the range operation of the order of 1 - 2 km for such systems. This fact in turn leads to application of such SUMMM for monitoring of pinnipeds mainly (taking into account the difficulty of the hanging of tags on mammal also).

However the important property of considered variant of the SUMMM is the opportunity of the organization of the telemetric system for transmission of main

physiological parameters of MM (pulse rate, respiration rate and so on). The observations of these parameters allows the direct relation between low-frequency sounds and physiological reaction of MM to be established.

For the second variant of the passive SUMMM when the MM signals are used, the low-frequency band is of main interest for an achievement the long range operation of. the SUMMM .

The above listed variants of the SUMMM have formed the basis for investigations at first stage of this work.

It is possible to use the active SUMMM for detection, localization, tacking and identification both of an individual MM and of their school. Here the application of an multistatic system with the distributed receiving array and the distributed radiating array is implied. However, in view of the action of the acoustic radiation on MM the given types of the SUMMM are not perspective ones and therefore they are not considered at this stage of works.

Nevertheless, the analysis of the active SUMMM variant is not ruled out in the following stages. For example, the active systems may be useful for monitoring of fish schools, invertebrate and plankton, and in neighbourhood of ice's edge. The last is the first section of the ecological chain under the study of adverse influence of low-frequency sounds on MM.

The creation of global surveillance system for monitoring of MM due to the progressive extending of the network of the local SUMMM shows large promise, in our point of view. The corresponding communication system for the interchange of information between local SUMMM and the information integration in unified site of surveillance is implied here. We hope to analyze in details the such a distributed surveillance system in the following stages of work.

Remarks.

Let us point some other opportunities of the SUMMM application.

It is possible to use warning signals for MM before the radiation of powerful low-frequency sounds. The choice of effective warning signals can made by the SUMMM.

Other application of the SUMMM may be connected with the control of moments of radiation in dependence on number of MM presented within the injury or annoyance zones.

2. THE BRIEF DESCRIPTION OF POSSIBLE MODELS OF SIGNALS AND NOISES FOR THE GIVEN ARCTIC REGION.

2.1. The type of radiated signals to be used with tags.

When the artificial signals from tagged MM are used in the SUMMM it is feasible to achieve several kilometers in range using the SUMMM.

Such SUMMM in supposed to solve several tasks.

Firstly, it is necessary to trace the dynamics of MM location. In many cases it is intersting to observe the interaction of several mammals. The solution of such a problem is complicated due to necessity of tagging different MM with different signal cues and simultaneous processing of the several signals. In addition the measuring of several physiological parameters of MM or external conditions characteristics can be produced. In this case the SUMMM has to perform both the trajectory measurements and the transmission of telemetric information.

If we limit ourselves by range of the SUMMM operation at about 1 km then the operating frequency band can be shifted in a region of several tens of kiloherz. However, here the requirements both of energetic optimality and of MM safety should be taken into account.

For the first task the radiated signals can be chosen as the periodical sequence of tone-pulses.

$$S_t(t) = \sum_k P_{Ot} \cos\left(2\Pi f_O t - \varphi_k - kT_S \right), \qquad (2.1.1)$$

Here $0 \le t \le \tau_t$, P_{Ot}, f_O, φ_k, T_s are amplitude, carrier frequency, initial phase and period of pulses repetition respectively. The receivers of signals can be incoherent. This allows to simplify the tags structure as much as possible. The tone pulse duration τ_t is defined by the required resolution capacity Δr:

$$\tau_t = \frac{\Delta r}{c}, \qquad (2.1.2)$$

here S ≈ 1500 m/sec is sound speed in sea water.

The period of pulses repetition must not be very little, because it can cause the ambiguity under the delays time difference estimation. The small period of pulses repetition leads to acceleration run out the battery of the acoustic source. On the other hand, the very long periods of pulse repetitions do not allow to control the details of MM trajectories.

We can choose the carrier frequency to separate individual mammals. If the used frequencies are in the limits of bandwidth Δf of electroacoustican transducer then there are no complications for the source implementation. However the processing algorithms are complicated because due to presence of many. The number of possible channels is determined by the bands Δf, $F_t \approx 1/\tau_t$, and by absolute values of Doppler deviation ΔF_d.

To simplify a receiver we can refuse from the Doppler deviation compensation and operate in the frequency band.

$$\Delta f_R = F_t \pm \Delta F_d. \qquad (2.1.3)$$

Here the accuracy of delay difference estimation (and consequently localization accuracy [2]) and output signal/noise ratio are lost. To avoid the losses in signal/noise ratio the another system of signals may be chosen. Here signal former is complicated, whereas the prosessing algorithm is simplified. It is not necessary to do the Doppler correction if the signal frequency band is much greater (say 10 times) then Doppler shift ΔF_d. The signals can be represented in this case in the form:

$$S_n(t) = \sum_k P_{On} \cdot n\left(t - kT_s \right), \qquad 0 \le t \le \tau_n, \qquad (2.1.4)$$

here τ_n is the pulse duration.

The algorithm of signal processing corresponds to the energetical receiver with further procedures of delays difference estimation. Here the product of the signal duration $\tau_n=\tau_t$ and frequency band $F_n>F_t$ is subject to condition:

$$B_n = \tau_n \cdot F_n > 1. \qquad (2.1.5)$$

Such signals belong to the class of noise signals and can be formed by phase manipulation of harmonical signal by binary pseudorandom sequence [3].

It should be pointed out that the number of signals with frequency band F_n and (nonoverlapping spectrums in frequency band Δf is less then for the case of the use of tone pulses.

We can use both tone pulses and pseudo-noise pulses to transmit limited amount of information from MM (simultaneously with decision of localization task). In this case it is necessary to radiate one or more frequency-shifted pulse sequences in synchronism with sequences of signals for localization coding the presence or absence of signals by for example binary or code.

Since the part (or possibly all) of signals separated in frequency will be used for the information transmission then number of separated mammals, is decreasing. In this case the source has to radiate the pulses in synchrony in several frequency bands and the practical implementation of power amplifier signal's former becomes complicated. Thus the simultaneous solution of localization and telemetry problems in the SUMMM causes both complication of autonomy radiating device on MM and complication of signal processing algorithms together with demodulation and decoding algorithms.

In most cases the conditions of multiray signal propagation in the hydroacoustical channel take place. The interference situation continuously changes, when the MM is in motion. In this case the signals with large base B should be used

for reliable transmission of telemetric information, where

$$B = F_B \cdot \tau_B \gg 1. \qquad (2.1.6)$$

For example, the signals recommended in work [4] can be chosen:

$$S_{Bm}(t)=P_{OB}\sum_{k=0}^{M-1}\cos\left[2\pi\left(f_O+\frac{k}{\tau_B}\right)t+\varphi_m(k)\right], \qquad 0\le t\le\tau_n, \qquad (2.1.7)$$

here P_{OB} is amplitude factor, f_O is the lowest frequency in the signal's spectrum, m=1,...,M - are numbers of signal, M is number of harmonic components of the signal. The phase manipulation $\varphi_m(k)$ of harmonic components is producing in accordance with a rule:

$$\sqrt{2}\ \exp\left\{\ i\varphi_m(k)\ \right\} = P_2(k)\ W_m^M(k) + iP_1(k),$$

here $P_1(k)$ is a binary pseudo-random sequence with length M, used for the measuring of hydroacoustical channel transfer function and receiver's synchronization; $P_2(k)$ - is a sequence which is orthogonal to $P_1(k)$, modulated by Walsh function W_m^M with length M. The number m of Walsh function determines a transmitted discrete message. The binary sequences $P_1(k)$, $P_2(k)$, $W_m^M(k)$ take the values to be equal to ±1.

In the systems of information transmission the adaptive processing of received signals may be realized by the use of these signals [4]. The resolution capacity for such systems is determined by signal frequency band. If the bandwidth F_B equal to several kHz then the resolution capacity is less then 1 metre. The signal duration can be chosen equal to period of MM trajectory reading (see (2.1.3)). In this case the radiation will be continious and this decreases irritation factor of the radiation for mammals. The simultaneous observation of several MM can be by realized by well known principles of Random-Access Discrete-Address System [5]. All signals

are radiated simultaneously. The separation of these signals is produced due to the distinction of the form of pseudo-random sequences which are used for the forming of corresponding signals in every transmitter.

2.2. Models of marine mammal signals.

The main acoustical characteristics of MM signals are included in the information bank of the program SUMMM-PAC (see chapter 4 of this volume) and the part of this bank is included in DEMO program which is delivered together with this volume. The information is concerned with the following MM. Pinnipeds, Common seal, Grey seal, Harp seal, Hooded seal, Bearded seal, Ringed seal, Walrus and others. Cetareans: Right whale, Blue whale, Fin whale, Minke, Humpback whale, Killer whale, Botlenose whale, White whale, Sperm whale, Killer whale and others (see [6,7]).

The results of our analysis of natural signals of Humpback whale is presented in the information bank also. The spectrum of Humpback whale signals is shown on fig. 2.2.1 (duration of Fourier analysis time window is about 0.2 sec). As it is seen from the figure there is one global maximum at frequency about 600 Hz but some not clearly expressed local maxima. The corresponding sonograms of Humpback whale signals are presented on figures 2.2.2 and 2.2.3. As may be seen from the figures, the frequency, which corresponds to maximum level of signal stays stable during several seconds. See Demo program for supplementary information.

A part of the information from information bank is presented in table 2.2.1 (pinniped) and table 2.2.2 (cetaceans).

Table 2.2.1

Pinniped.

Mammal	Form of signal, frequencies	Maximal source level
1. Common seal	1. Impulse series with basic frequency less then 1 KHz. 2. 3 separate sounds with basic frequency less then 38 kHz and 4-7 harmonics.	140-150 dB re 1 mkPa at 1 m range
2. Grey seal	Impulse signals with frequency 12 kHz, intervals between pulses in pairs 0.01-0.2 S, and repetition rate in series 70-80 pulses per second.	-
3. Harp seal	The basic signal range 0.5-10 kHz and their duration can vary from 0.12 sec to several seconds.	-
4. Hooded seal	1. Clicks in the frequency range 0.1-16 kHz with different basic frequencies. 2. Low frequency range of 0.1-12 kHz and with harmonics up to 3-6 kHz.	-
5. Bearded seal	Frequency modulated warbles of 1 min duration dropping in frequency from 2-3 kHz to 200 Hz.	-

Table 2.2.1.

Mammal	Form of signal, frequencies	Maximal source level
6. Ringed seal	1. Single and puired pulsed signals in the frequency band up to 4 kHz with the intervals between the signals in pairs 2-20 msec. 2. Basic frequency in the range of 1-3 kHz and harmonic constituents up to 6 kHz. The signal duration varies within 0.2-0.5 sec.	-
7. Walrus	1. Series of clicks of 0.015-0.02 sec in duration with the basic frequency of 400 Hz. 2. Powerfull bell-like sounds of frequency 0.4-1.2 kHz and duration 1-1.5 sec. 3. Gnashing starting with 4-10 pulses, each of them having basic frequency at 400-600 Hz and duration 0.1 sec.	-

Table 2.2.2

Cetaceans

Mammal	Form of signal, frequencies	Maximal source level
1. Blue whale	1. Mean dominant frequency at 90 Hz and pulse inclusions of 20-2000 Hz. 2. Harp broadband sounds produced during the spring migration in the frequency range 100-3500 Hz. 3. Low frequency and frequency modulated screams in the frequency band of 12-200 Hz and duration 36.5 sec.	175-185 dB
2. Fin whale	Series of pulses of dropping frequencies (23-18 Hz).	186 dB
3. Sei whale	Click series (7-10) having the maximum energy at a frequency of 3 kHz.	-
4. Killer whale	1. Whistles of the basic frequency 15-18 kHz and duration from 50 ms to 10-12 sec. 2. Pulse screams of frequency 1-6 kHz and duration from 50ms to 10 sec.	-

Table 2.2.2.

Mammal	Form of signal, frequencies	Maximal source level
5. Humpback whale	1. Low frequency screams in the frequency range 120-800 Hz of 0.5-1.5 S duration. 2. Screams of higher frequencies (4-8 kHz).	124-155 dB
6. Monodon monoceros	Narrow-band spectrum; dominant frequency peak is at 40 kHz and the second smaller peak at 20 kHz.	200-218 dB

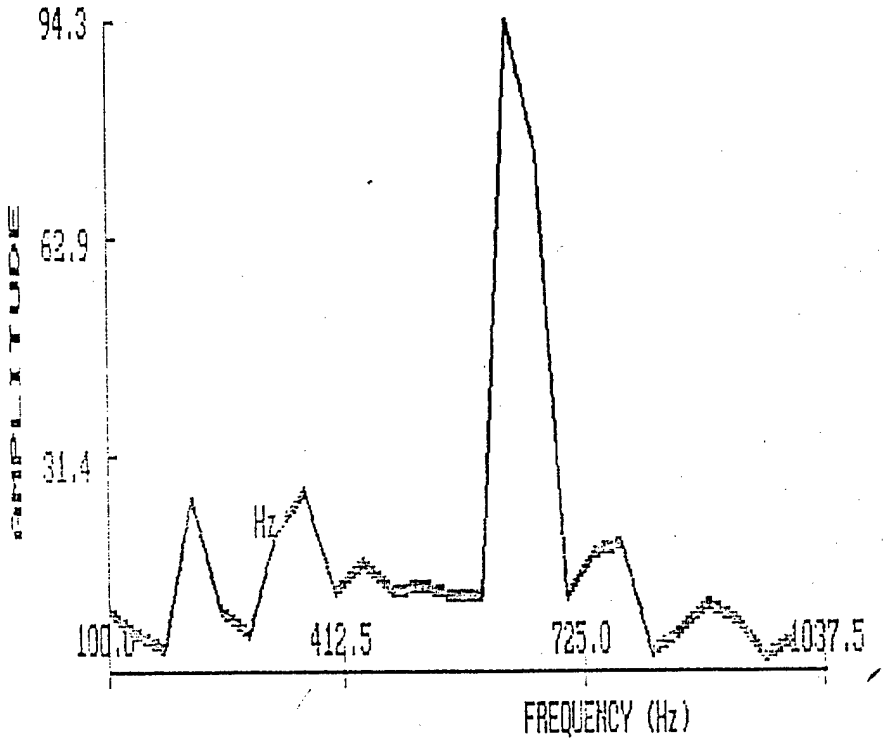

Fig. 2.2.1. Humpback whale signal spectrum.

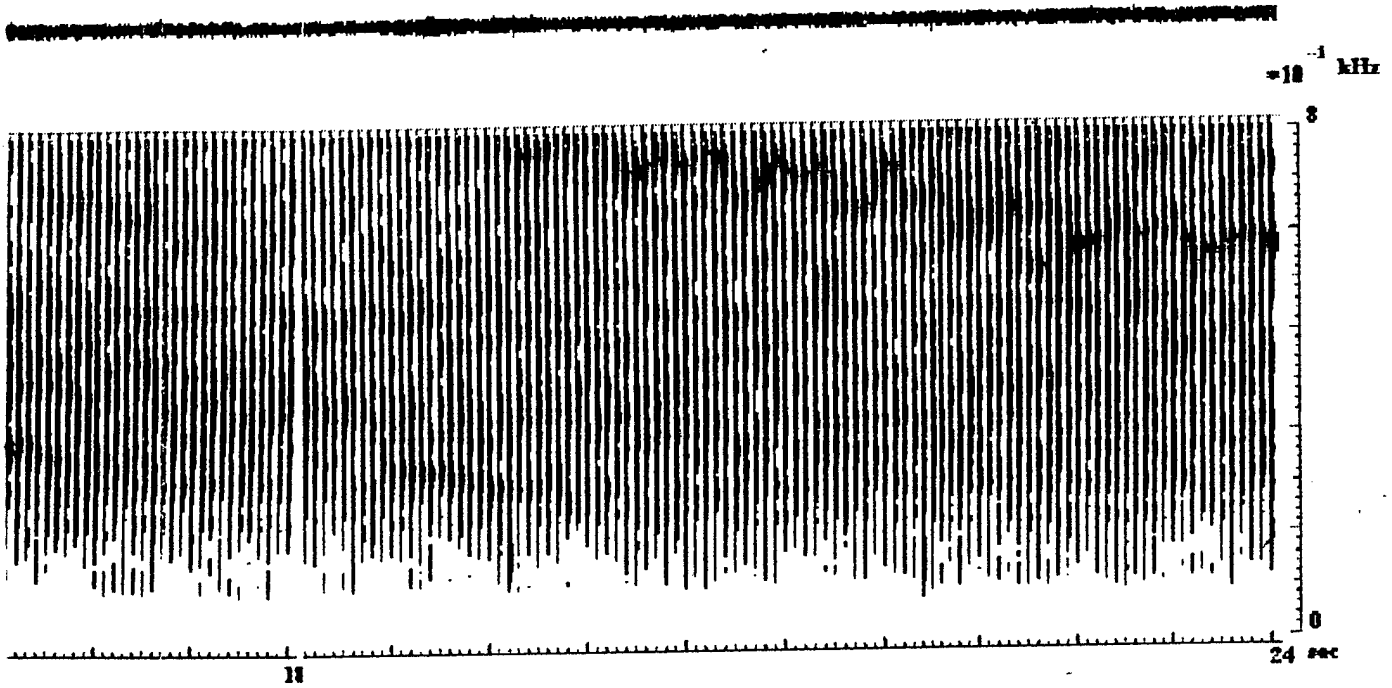
$\pm 10^{-1}$ kHz
8
0
24 sec
11

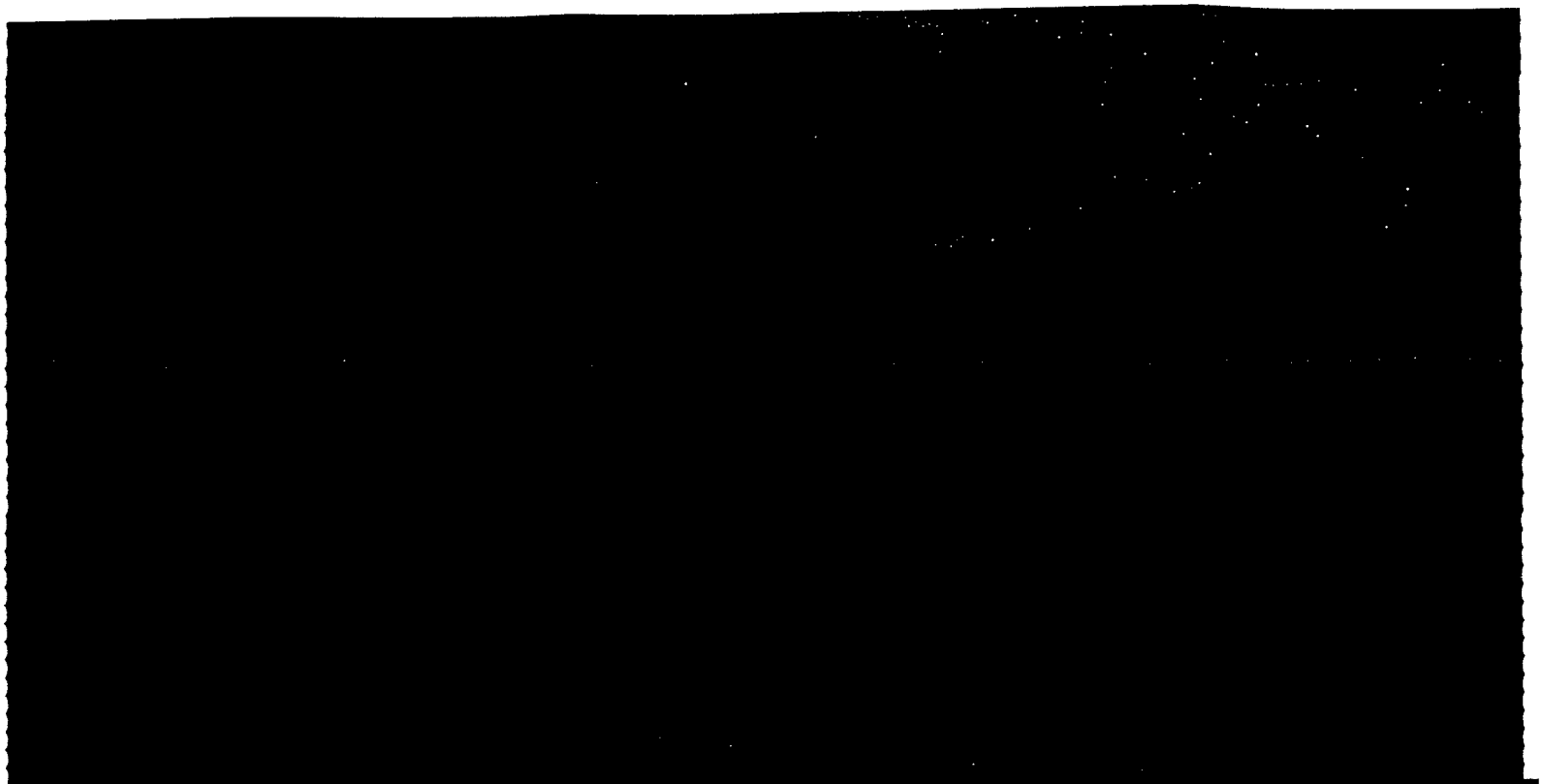

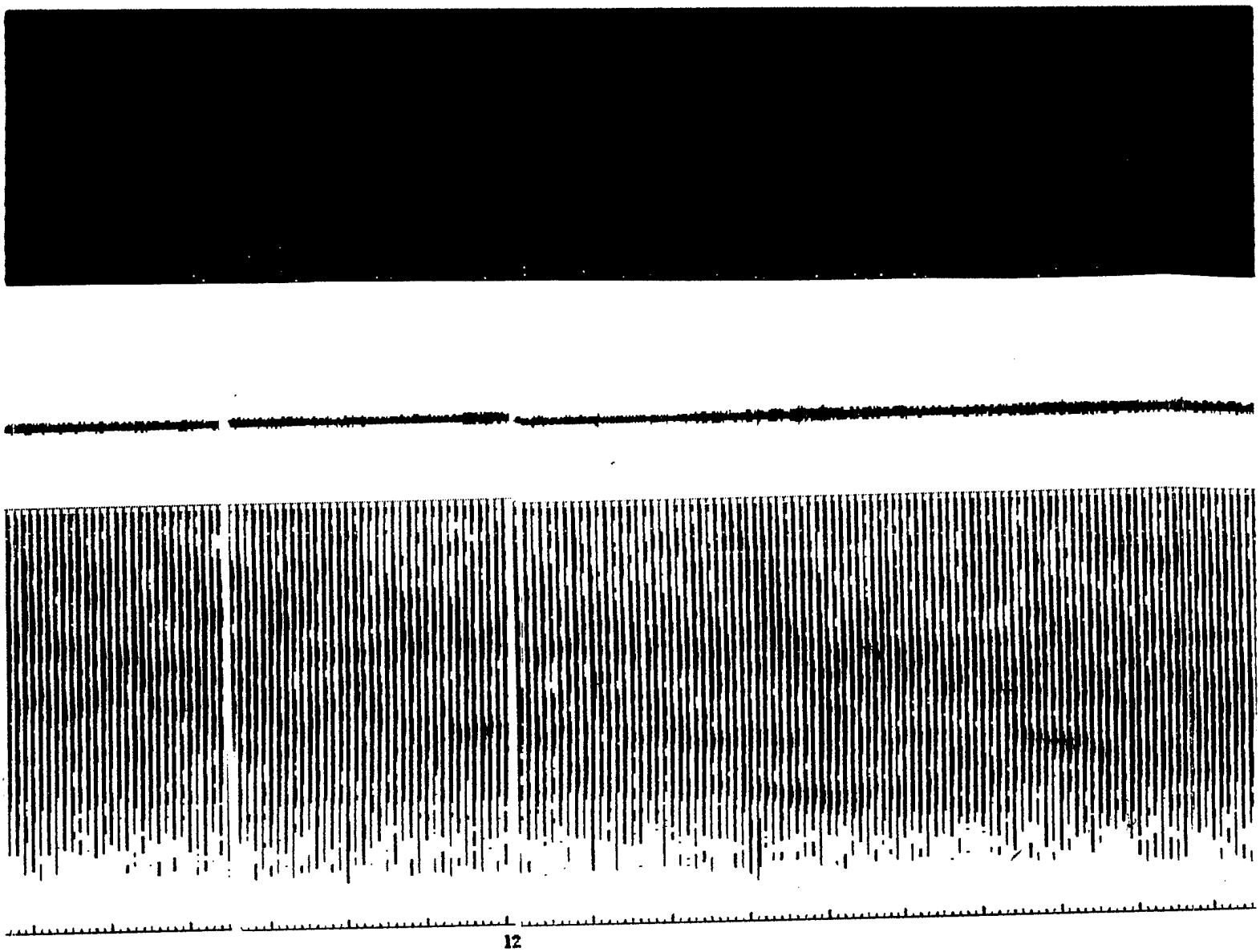

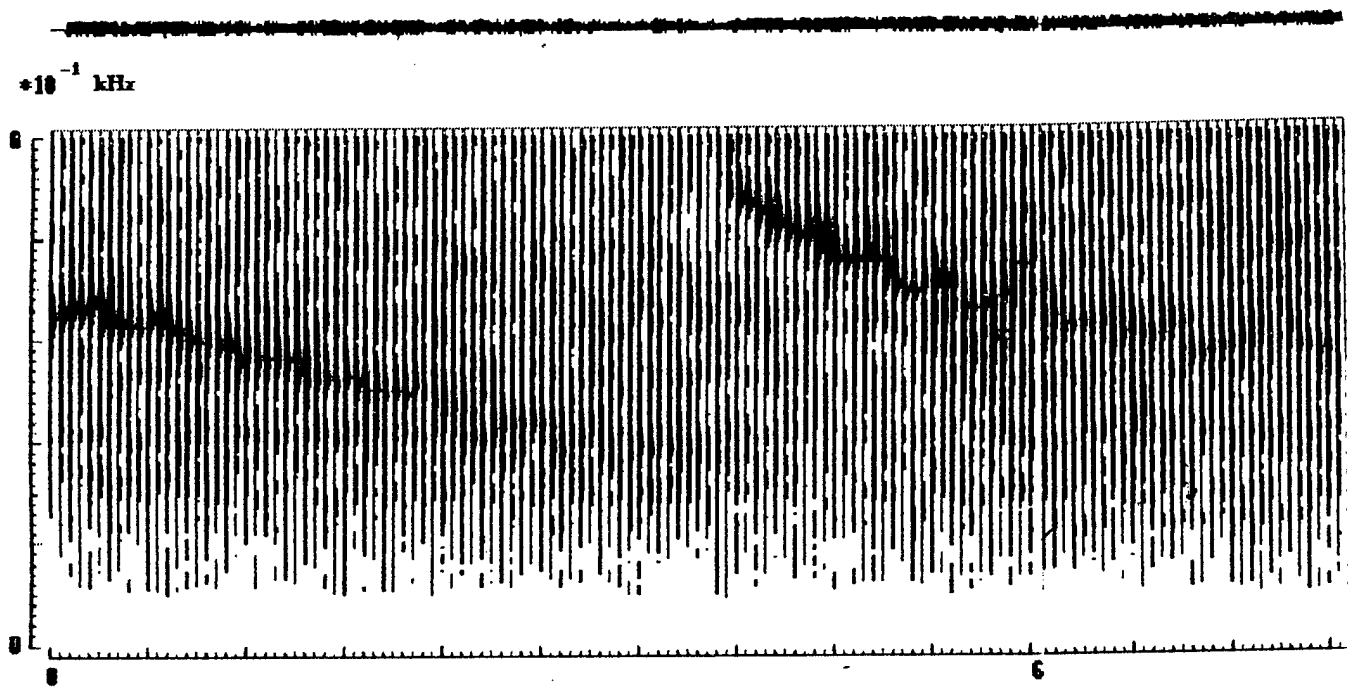

Fig. 2.2.2. Sonogram of the first Humpback whale signal.

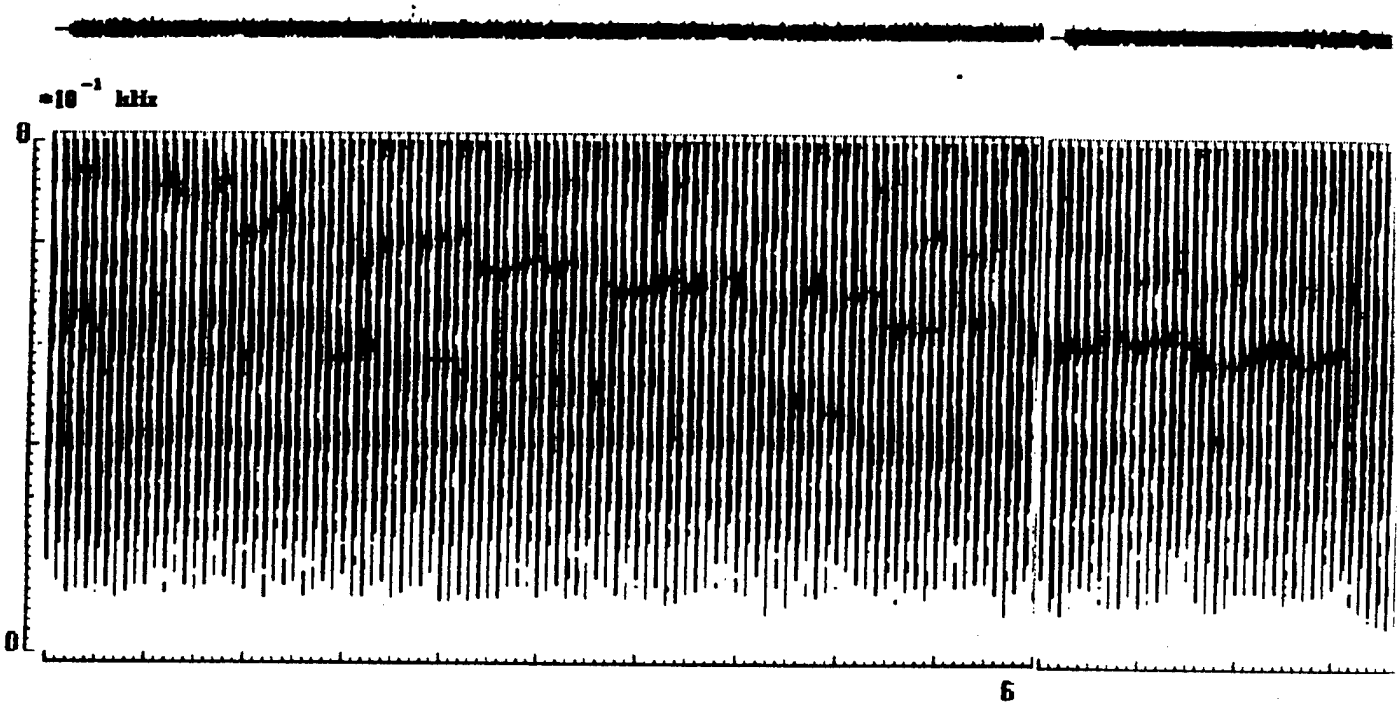

Fig. 2.2.3. Sonogram of the second Humpback whale signal.

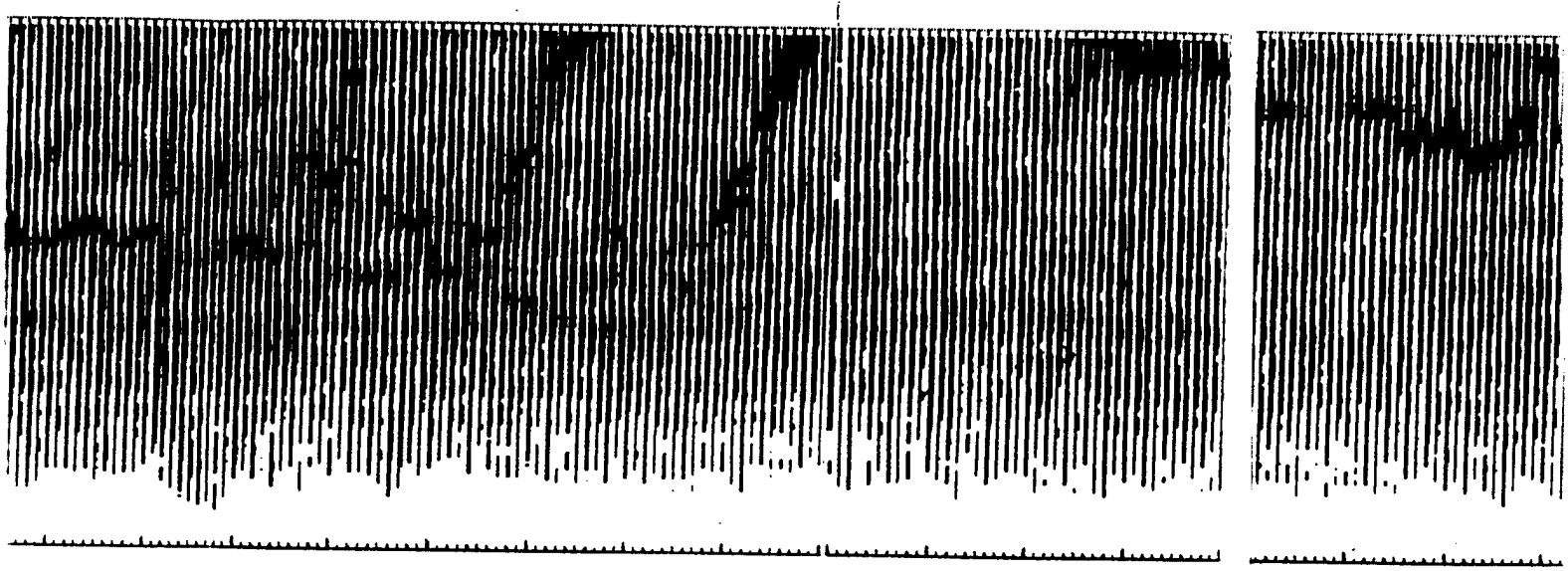

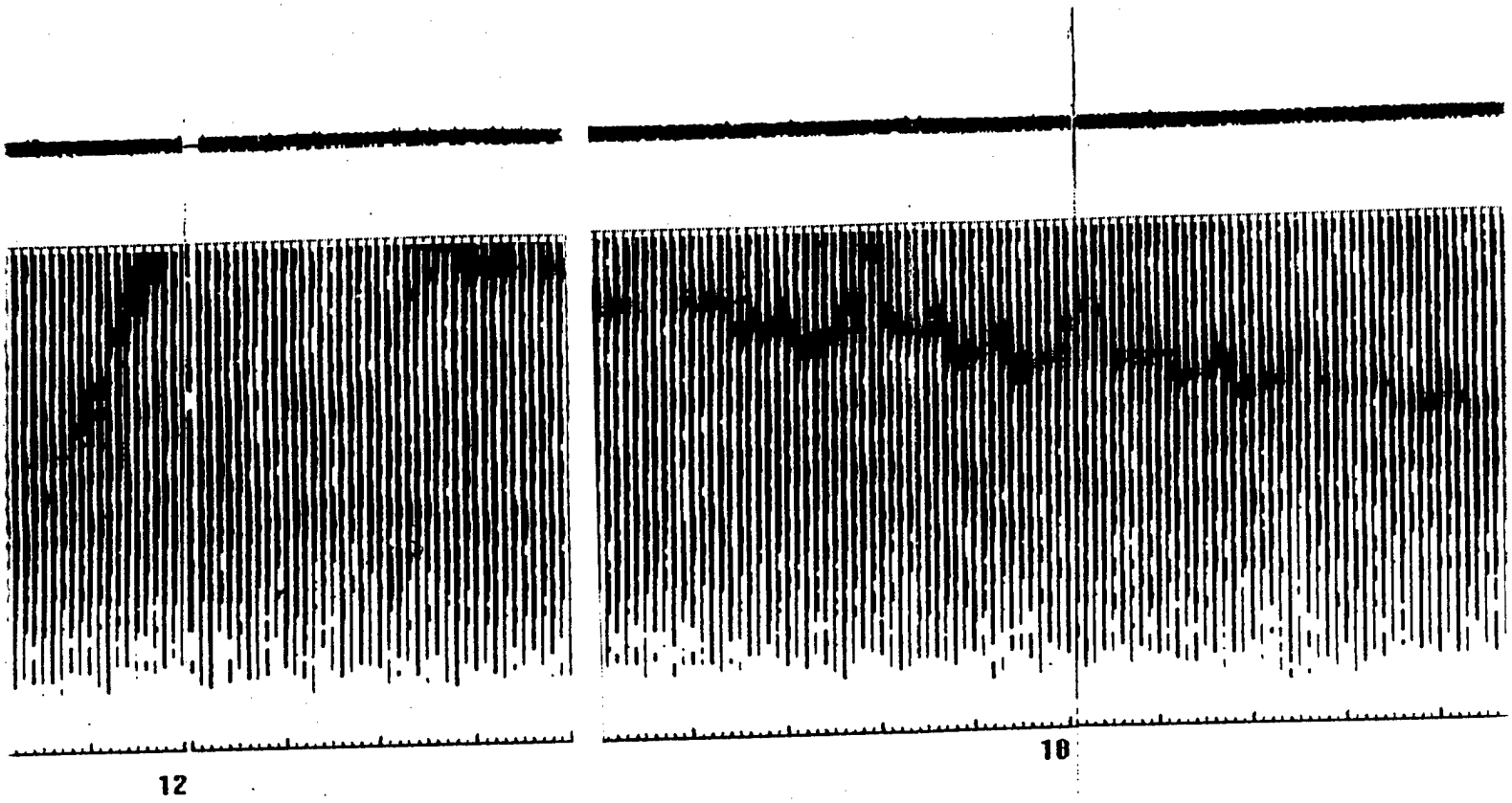
12
18

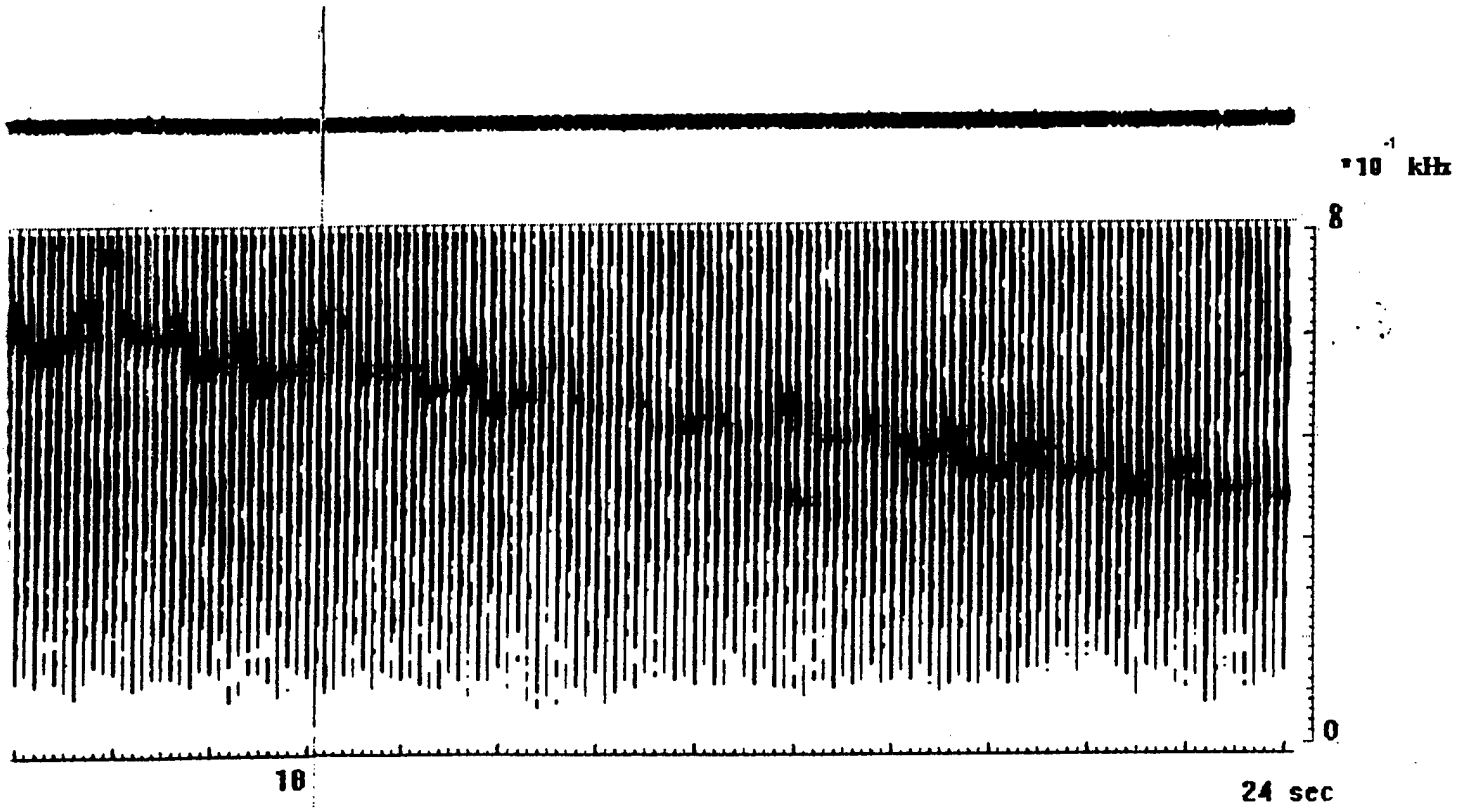

4

2.3. Signal propagation in the given Arctic region.

2.3.1. Characteristics of the region.

The region is over lain by underwater canyon Litke Norther Thou Spitbergen with central point 83^0 of North latitude 30^0 of East longitude.

This point is located at approximately 150 miles from coastal line. The rising Ermak plateau (depth of order 600 m) occurs at 180 miles to South West from the central point. Deep-water mountain ridge Hankel extends in the North direction, the hollow Nansen extends to the North-East direction for some thousands miles. The depth of the sea in the neighborhood of the central point is 3000 m. The depth is rapidly grown up to 3500 m to the North and to the North-East. Isobath at 1000 m occurs at 90 miles from the central point to the South and at 110 miles - to the South-West.

The bottom is strongly dismembered under the central point, however it is further changed to flat plains which are transformed to wave plains. The slopes of the rising Ermak platean is strongly dismembered. The gentle slope in the South direction is weakly dismembered and then as far as North-East Land the slope is transformed to the plain with small scaled and small blocked dismembering. The bottom consists of clay silts which lay on sedimentary rocks. The thickness of sediments is some thousands meters. The velocity of longitudinal waves is 1700-1800 m/sec whereas the velocity of shear waves is not more then 300 m/sec. Velocities of currents in the region averaged over year are not more then 2 m/sec [20]. In the vicinity of the surface currents currents are directed to North-East and to East. At a depth of 100-1000 m the directions is to North-West and to South-West. The variations of water level in response to flows are up to 1.5 m at semidiwinal period.

Most of the time the region is covered by ice. Only in September the boundary

is interfaced by flatting ice lines up in the South part of the region. The central and the North parts of the region are covered by ice for entire year. Resulting drift of ice (from North-East to South-West) is of order 1000 km per year. The velocity of the drift is maximal in winter and is minimal in summer.

In response of ice melting salinity of water is decreased. The fresh waters are gathered in upper layers spaced the vicinity of the ice-water interface where the concentration of salt decreases up to 30.5-31 $^{0}/_{00}$. The Atlantic waters with the concentration of salt 34.5-35 $^{0}/_{00}$ are gone to greater depth. The Atlantic heat of the region is grouped at middle depth. The annual average temperature of water is positive in the layer from 200 m to 800 m and decreased in Northern direction. This fact produces the characteristic dependence of sound speed on depth (see Fig. 2.3.1). The water layers spaced in the vicinity of the ice with negative temperature produce the sound channel with axis at the surface and with vertical gradient of sound speed equal to 130 m/sec per 1 km. The thickness of the channel extends in Northern direction from 100 m at latitude 80^{0} to 250 m at latitude 88^{0}. In the middle depth the hydrostatical gradient is partly compensated by the high temperature of water. As a result the one is decreased up to 10 m/sec per 1 km. At greater depth (> 750 m) where the water temperature is again decreased the gradient is increased up to 15 m/sec per 1 km.

The given profile is supported by repeated immediate measurements which are carried out in the Arctic expeditions of the Acoustics Institute of in cooperation with the Arctic and Antarctic Institute . As example of the dependence of sound speed, on depth the corresponding measurements (summer 1974) are given in the Tab. 1. These measurements are carried out in three points:

on meridian 15^{0} East longitude at ranges 100 km, 200 km, 300 km from parallel 80^{0} Vorth in direction to North pole.

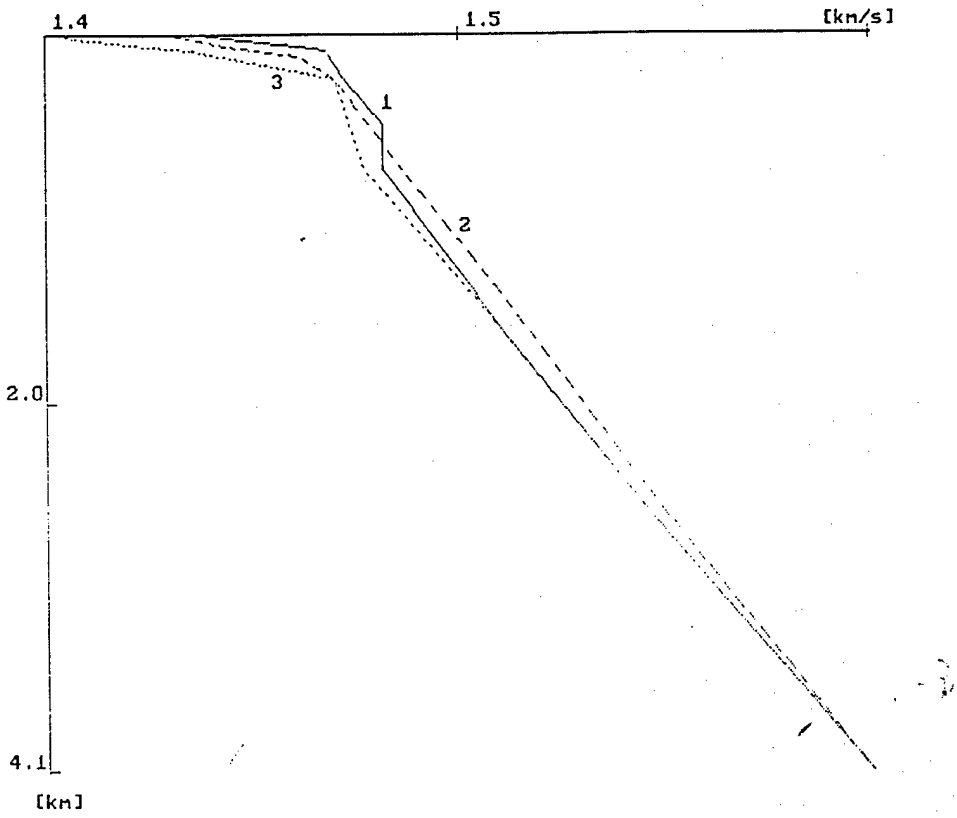

Fig. 2.3.1. Sound speed profiles for different latitudes.

1 - 80^0 of north latitude

2 - 84^0 of north latitude

3 - 88^0 of north latitude.

The measurements of c(z) in upper layers of water were carried out in April 1994 in the experiment under supervision of Dr.P.Mikhalevsky where the scientists of the Acoustics Institute and of Institute of the Institute Applyed Physics have taken part in the experiment in parallel with American and Norvegian scientists.

The plots of temperature, salinity and sound speed versus depth is presented in Fig2.3.2. These dependences are measured during 17.04.94 at the point $83^0 57'$ Vorth, 27^0 East . The values of salinity and temperature according to [20] are markad by black squares. The good agreement of experimental and averaged data allows the dependence c(z) presented in Fig. 2.3.3 to be used as typical for given regions.

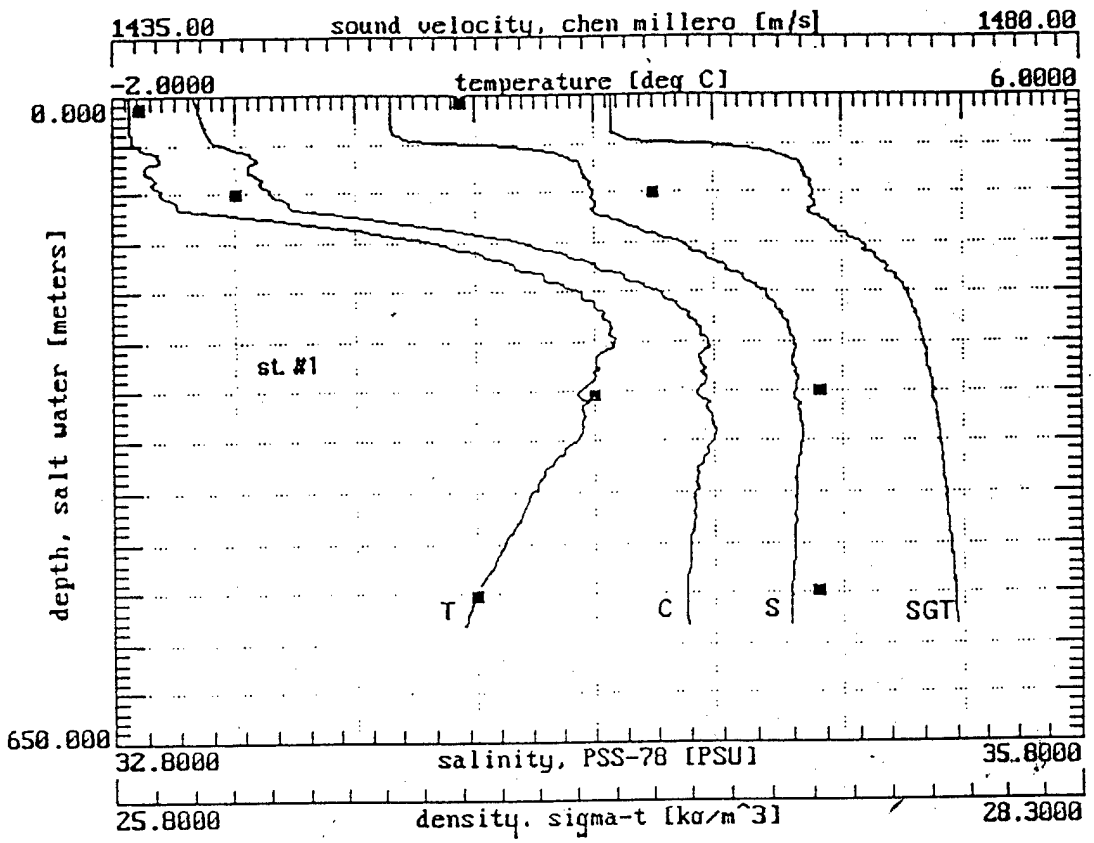

Fig. 2.3.2. Temperature, salinity, sound velocity and density profiles measured 17.04.94 at the point $83^{0}57'$ North , 27^{0} East. Black squares indicate the results of calculations [20].

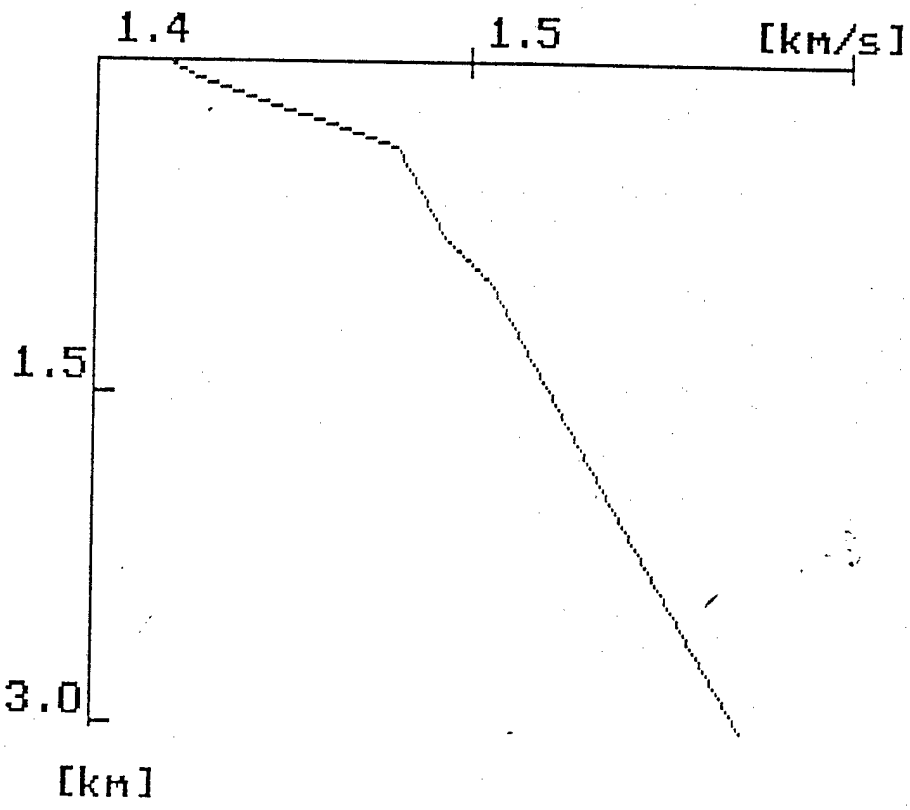

Fig. 2.3.3. Typical c(z) profile.

Acoustical characteristics of ice cover.

For given region the yearly ice with mean thickness 1,5 ÷ 2 m is predominant one. The root-mean-square (RMS)height of the roughness of lower boundary is σ = 1 m ÷ 1,5 m whereas the radius of spatial correlation ρ_0 = 20m ÷ 25m. In parallel with the yearly ice the along - standing ice with the mean thickness being approximately equal to 4m the RMS height of roughness - $\sigma \simeq 3$m and the radius of correlation - ρ_0 = 40m is existing in the region also. In addition hummocks occupy 4.5 % of ice cover. The mean value of hummocks (draught is as much as 8.4m and the RMS value of height is 1.65 m.

The characteristics of ice are spatially inhomogeneous and depend on the season. In summer the velocities of longitudinal waves are varied within 2900 - 3300 m/sec, in winter - are within limits 3200-4000 m/sec. In summer velocities of shear waves are varied within limits 1500-1650 m/sec and in winter - within limits 1600-1850 m/sec.

The attenuation of the sound in ice is dependent on frequency. At the frequencies lower than 0.5 kHz the attenuation of longitudinal waves Δ_e is varied within 0.08-01 dB/m and that of shear waves Δ_t is two times greater than one. At frequencies higher than 0.5 kHz attenuations Δ_e, Δ_t are determined by the expressions:

$$\Delta_e(\text{dB/m}) = 0.4 + 0.04 \cdot f \ (\text{kHz})$$

$$\Delta_t(\text{dB/m}) = 0.705 + 0.023 \cdot f^2 \ (\text{kHz}).$$

There is good reason to use the complex mean values of sound speed for the calculations of the reflection coefficient V_0 from even ice with consideration of attenuation at low frequencies. In summer velocity of longitudinal waves is $3100 \cdot (1 - i \cdot 0.002)$ m/sec, whereas in winter one is $1800 \cdot (1 - i \cdot 0.08)$ m/sec.

Table 2.3.1.Depth dependence of sound speed .

Z [km] \ R [km]	100	200	300
0	1439.2924	1439.3365	1438.3389
10	1439.3024	1439.3465	1438.6178
25	1439.8312	1439.4767	1438.7132
50	1439.9083	1439.9525	1439.3333
75	1440.4401	1441.2786	1441.7513
100	1444.1863	1449.3263	1444.6186
150	1458.2719	1457.1223	1450.8282
200	1462.3858	1458.6772	1456.3909
250	1463.3284	1460.0147	1458.3867
300	1463.5051	1460.7243	1459.3626
400	1463.9282	1461.3183	1460.4101
500	1464.6558	1462.1969	1459.8870
750	1463.7823	1460.6457	1461.5292
1000	1464.2624	1463.1898	1463.9560
1250	1466.5691	1466.6768	1467.2532
1500	1470.6441	1470.4212	1470.8584
2000	1478.7941	1478.4093	1478.6118
2500	1486.9441	1486.5593	1487.0388
3000		1494.7093	1495.8802
3500		1502.8593	1505.0435
4000			1513.1935

R - range between the point with 80^0 North latitude,

15^0 East and North pole,

Z - depth.

The measurements of the reflection coefficient from rough ice V at frequencies below or equal to 0.5 kHz have demonstrated satisfactory agreement of the experimental results with theoretical ones which can be obtained by the formula:

$$|V| = |V_0| \cdot e^{-p^2/2}$$

where $P = 2 \cdot k \cdot \sigma \cdot \sin \cdot \varphi$ is Rayleigh's parameter, φ is grazing angle, k is the corresponding wavenumber.

There is need to consider the layered structure of ice at frequencies higher then 0.5 kHz. The reflected sound field is appreciably noncoherent at large values of φ. When φ tends to 0^0 and the frequency of sound is scaled down the field coherence is increased. The coefficient of reflection for summed field weakly depend on frequencies within the range 1 kHz to 10 kHz.

Backscattering force M is another important characteristics of the ice when the active SUMMM is considered. Backscattering force depends on the type of ice, the frequency of sound and the grazing angle of the sound ray. In particular, for the yearly ice at frequency 1 kHz and $\varphi=15^0$ the M occurs in the range - 35 - 40 dB and at $\varphi=70^0$ is in the range - 17 ÷ -21 dB. That is M is essentially increased with the increasing of φ. At frequencies below 1 kHz M is lowered with the increasing of frequency and at frequencies higher than 1 kHz M weakly depends on frequency. In summer M is several dB less than in winter.

2.3.2. Sound propagation in the Arctic waveguide.

The near-ice sound channel (Fig.2.3.3) with thickness of about 200 m holds the rays with the grazing angles in the vicinity of the surface lying in range from 0^0 to 8^0 approximately. The rays with greater grazing angles go to greater depth and

returns to surface at a range of 20 km ÷ 50 km from the sound source.

If the source is not directional then the shallow water rays and the deep water rays (nonreflected from bottom) are approximately of the same energy. In near-ice layer the density of energy is larger than in the deep water because of the thickness of near-ice layer less than the thickness of the ocean. However the sound propagating along sloping rays is attenuated more rapidly than along deep water rays due to sloping rays are often in contact with the rough ice boundary. So the deep water sounds are dominated at large ranges. The methods of sound field calculation developed the in Acoustics Institute are presented in [23-25]. The example of anomaly calculation (in relation to unlimited space) of the levels for regular and scattering components of the sound field at frequency 60 Hz as a function of range is presented in Fig. 2.3.4. The depth of the ocean is 3000 m.

The source and the receiver were placed at 100 m in the near-ice layer. The bottom was considered as liquid with the density of 2 g/sm^3 and with the sound speed equal to $1850 \cdot (1 - i \cdot 0.005)$ m/sec. The square of the ice cover of 70 % was chosen as two yearly ice with the mean thickness h = 2.5 m, the roughness standard deviation σ=1.3 m and the radius of correlation ρ_0=100 m. The along-standing ice with h=4.1m, σ=2.7m and ρ_0=40m formed 30 % of the total. The velocity of longitudinal wave in the ice V_e is equal to $3100 \cdot (1 - i \cdot 0.02)$ m/sec, velocity of shear wave is $V_t = 1800 \cdot (1 - i \cdot 0.05)$ m/sec. The fig. 2.3.4 shows the anomaly of total field (marked by figure 1) and its coherent component (marked by figure 2) versus distance. Curve marked 3 corresponds to the coherent component of the field in the near-ice layer and one marked by 4 is coherent component of the field in the deep water layers. It can be easily seen that the anomaly of the deep water signals is increased whereas the anomaly of the shallow water signal tends to zero at ranges of order of hundreds km. The coherent component consists of the deep water signal at the distances that are more than 500 km. The propagation in the wave guide is worse than in unlimited space

at the distances more than 1000 km.

The anomaly is decreased with the increasing of frequency. The corresponding curves for given waveguide are presented in Fig.2.3.5. Fig.2.3.6 shows the coefficient of coherence. On Fig.2.3.7, Fig.2.3.8 the dependence of attenuation coefficients of versus frequency is shown for the given waveguide and above mentioned location of a source and a receiver in the near-ice layer. Fig.2.3.7 corresponds to total field whereas Fig.2.3.8 corresponds to its coherent component. The curve 1 corresponds to the shallow water signals, curve 2 is to the deep water signals, curve 3 is to the total field. The curve 4 shows the absorption in the water as a function of frequency. The data presented in [18] is marked by crosses in Fig.2.3.7. As it is seen from Fig. 2.3.7, the ones are satisfactory correlated with the curve for total field which consists of shallow and deep water field.

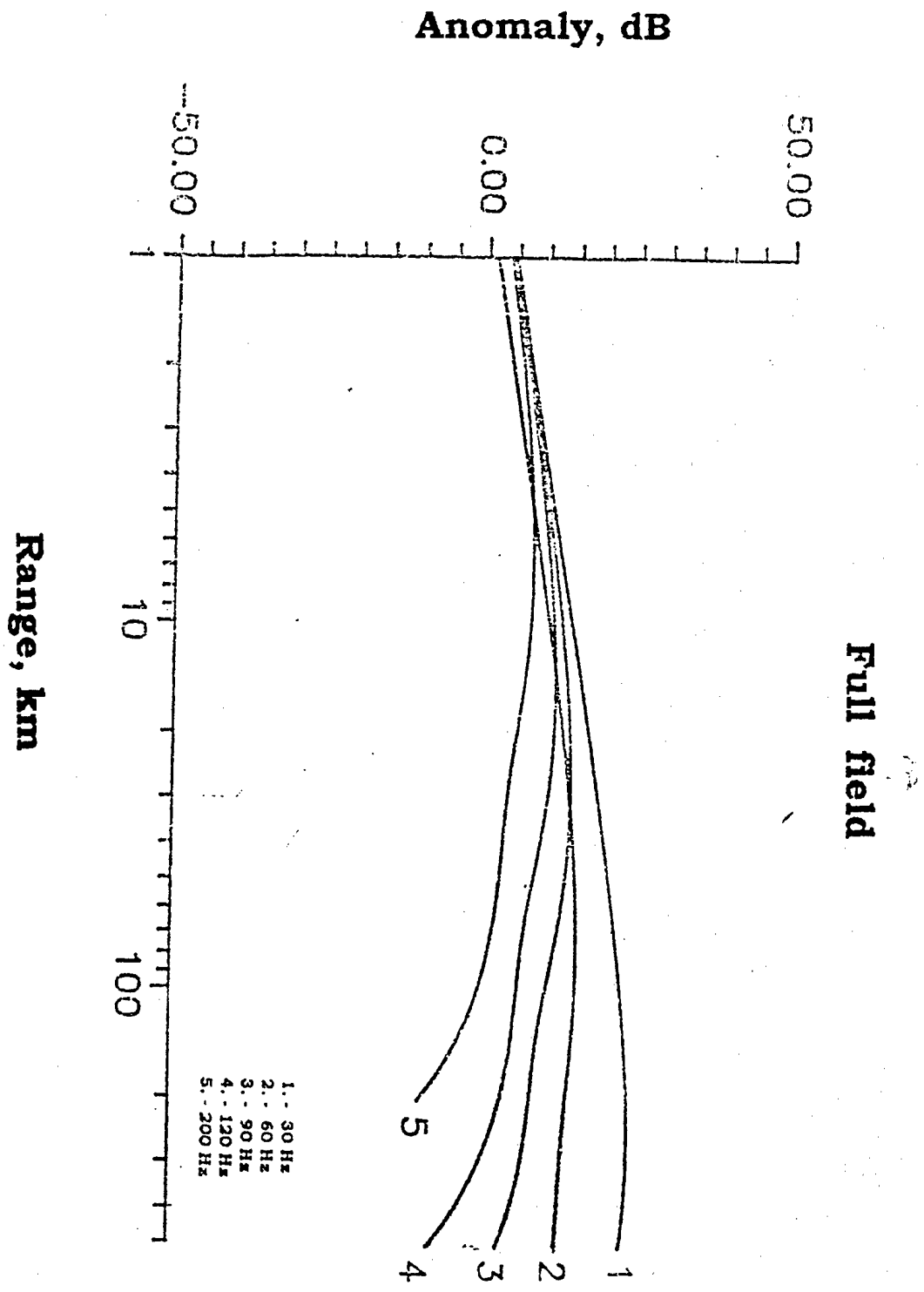

Fig. 2.3.5. Anomaly of the full field at different frequencies.

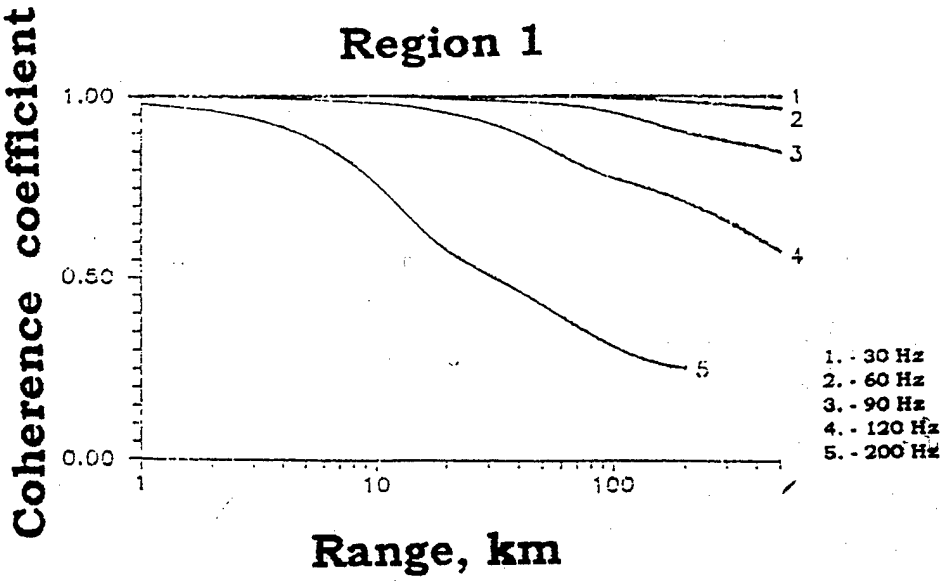

Fig. 2.3.6. The part of the coherent field energy

(coherence coefficient).

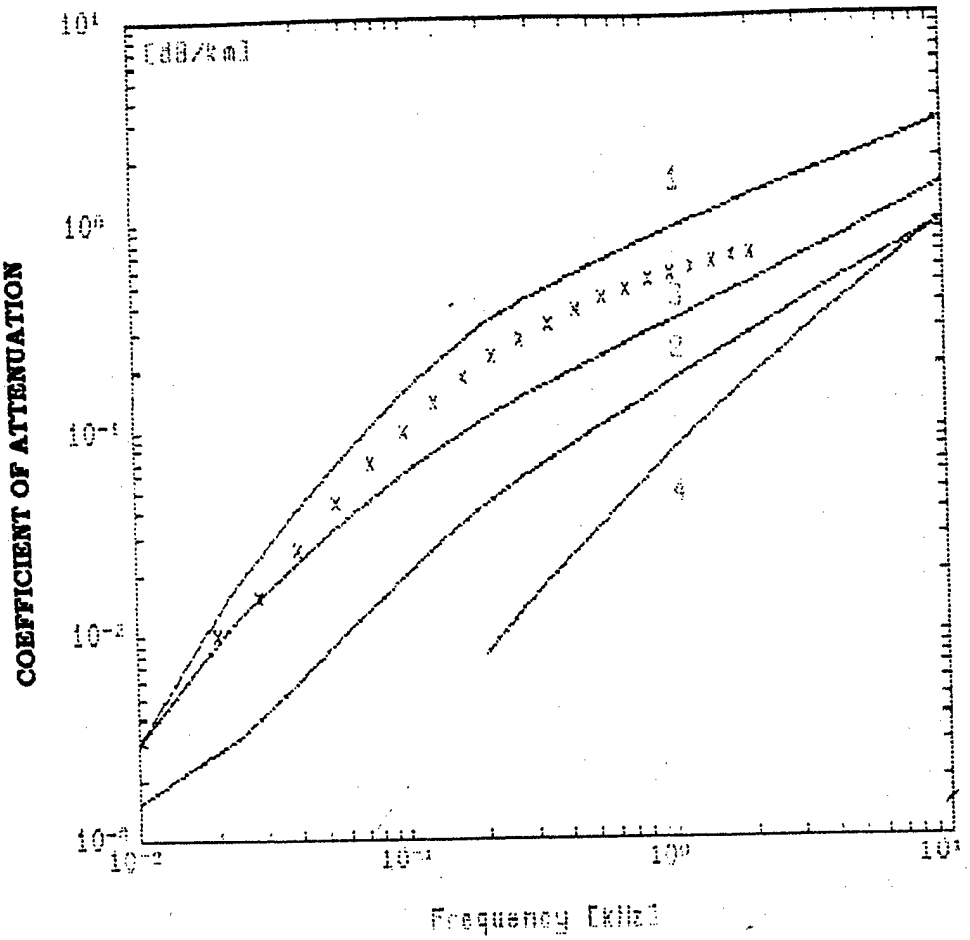

Fig. 2.3.7. The attenuation coefficient of the full field

1 - signals propagated

in vicinity of the ice cover;

2 - deepwater signals;

3 - summed field;

4 - the absorption in the water; the

crosses indicate the results presented in [18].

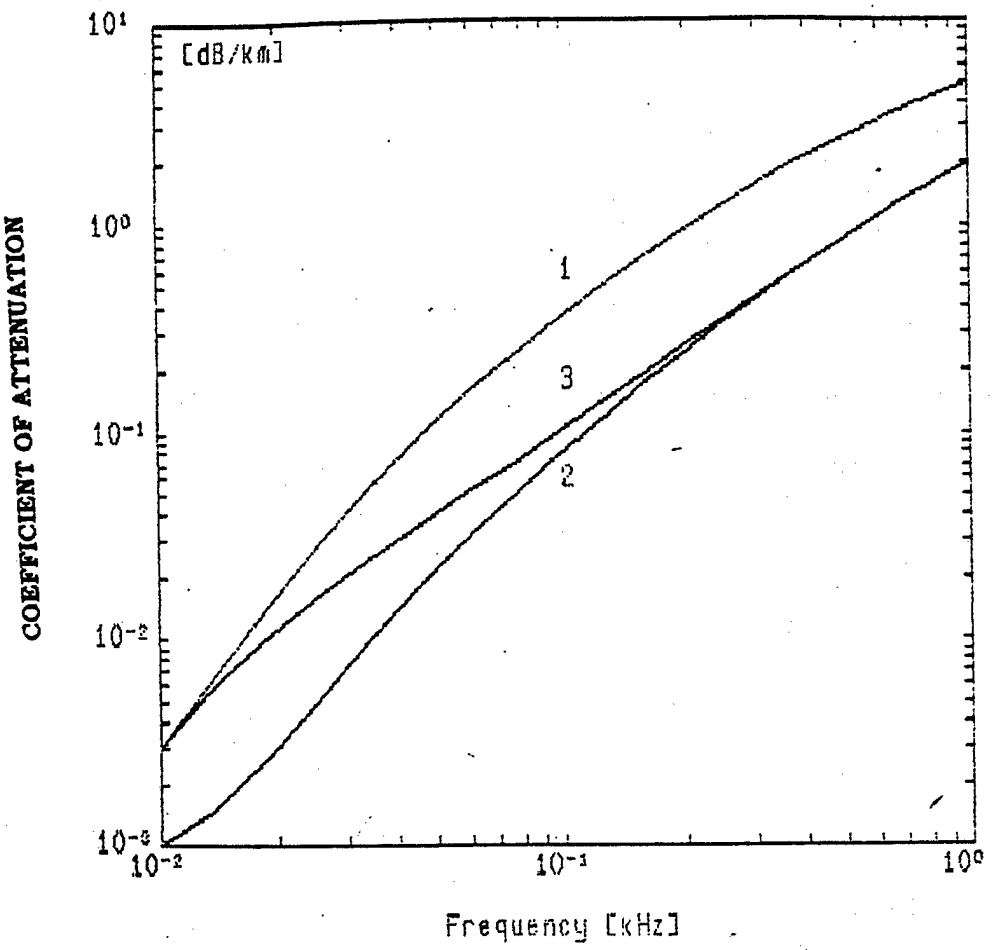

Fig. 2.3.8. The attenuation coefficient of the coherent field

1 -the signals propagated in

the vicinity of the ice;

2 - the deepwater signals;

3 - summed field.

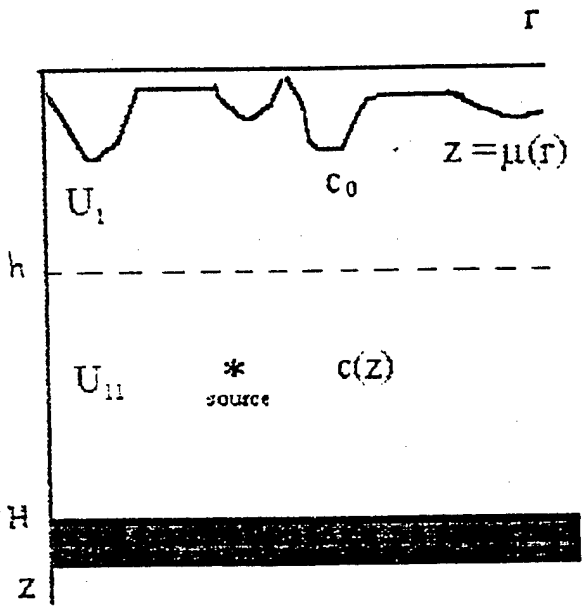

Fig. 2.3.9.

2.3.3. Theory.

Investigation of sound propagation of near the ice cover requires consideration of scattering of sound waves by rough boundary liquid-solid . As a rule in this case the shape of rough boundary is described by random function which depends on spatial coordinates. So the problem should be treated as statistical problem which intended to predict statistical characteristics of scattering field (distribution functions, statistical moments, correlation function etc.) by known statistical characteristics of rough boundary. To get the characteristics of scattering field, the most commonly is used perturbation theory and Kirchgoff approximation [28, 29]. However these methods are limited by conditions imposed on the scale of roughness and the frequency of radiating signal. As noted in [26], the shape of lower ice boundary is imperfectly understood, so the question of feasibility of perturbation theory or Kirchgoff approximation may be involved. To circumvent these difficulties we used one possible approach based on the assumption that repeated reflections of sound field from rough boundary are uncorrelated [27]. It can be justified when the scale of roughness correlation is much less than minimal length of the ray cycle coming to a receiver. Under known limiting cases uncorrelated reflections approximation leads to perturbation theory or to Kirchgoff approximation.

At this stage, we have concentrated on the first statistical moment of scattering field. Let us consider water layer enclosed by two impedance boundaries as a model of the hydroacoustic waveguide (Fig.2.3.9). The upper rough boundary ice-water described by stochastic equation $z=\mu(\bar{r})$ in the neighborhood of the level z=0. Random function $\mu(\bar{r})$ is gaussian one with mean $<\mu(r)>=0$ and correlation function $<\mu(r)\ \mu(r')>=\sigma^2 B(r-r')$. The quantity σ is the mean square deviation of roughness near the level z=0. Relative impedances of upper boundary Z_0 and lower boundary Z_H are

independent of horizontal coordinates $\bar{r}=(x,y)$. Homogeneous water layer (sound speed c_0) of thickness h exists near boundary ice-water as experimental data show. Below the layer $\mu(r)<z<h$ there is inhomogeneous water (sound speed c(z)) at $h<z<H$. In this case we can write out sound fields U_I and U_{II} in layered homogeneous and layered inhomogeneous media correspondingly which satisfy continuousness conditions and take the limit at $h\to 0$ in boundary condition for the first statistical moment of scattering field $\langle U\rangle$ inciuding c_0 in c(z).

Let us assume that there is a point source of harmonic oscillations at frequency ω located at the point $(\bar{r}_0,z_0)$ (Fig.2.3.9). From Green's theorem it follows:

$$U_I(\bar{r}_1 z;\bar{r}_0,z_0)=\int \frac{d^2p}{(2\pi)^2}\cdot e^{i(\bar{p},\bar{r})}\cdot\left[A(\bar{p}|\bar{r}_0,z_0)\cdot e^{-i\kappa z} + \frac{1}{2i\kappa}\cdot \right.$$

$$\left.\cdot V(\bar{p}|\bar{r}_0 z_0)e^{i\kappa z}\right], \qquad (2.3.1)$$

where

$$V(\bar{p}|\bar{r}_0,z_0)=\int d^2r dz\cdot e^{-i(\bar{p},\bar{r})-i\kappa z}\cdot\delta(z-\mu(\bar{r}))\cdot\left[-Z_0(z) + +i\kappa - i(\bar{p},\nabla\mu(\bar{r}))\right]\cdot U_I(\bar{r},z;\bar{r}_0,z_0),$$

$$\kappa=\sqrt{\frac{\omega^2}{c_0^2} - |\bar{p}|^2}\ ,\ d^2r=dx\cdot dy,\ d^2p=dp_x\cdot dp_y,\ |\bar{p}|^2=p_x^2+p_y^2,$$

$A(\bar{p}|\bar{r}_0,z_0)$ is coefficient which is determined by contentiousness conditions for the fields U_I, U_{II} at z=h.

The field U_{II} may be written by Fourier transform as

$$U_{II}(\bar{r}_1 z;\bar{r}_0,z_0)=\int \frac{d^2p}{(2\pi)^2}\cdot e^{i(\bar{p},\bar{r}-\bar{r}_0)}\cdot u(z,z_0,\bar{p}), \qquad (2.3.2)$$

where

$$u(z,z_0,\bar{p})= \frac{\varphi_1(\bar{p},z)\varphi_2(\bar{p},z_0)\vartheta(z_0-z) + \varphi_1(\bar{p},z_0)\varphi_2(\bar{p},z)\vartheta(z-z_0)}{\varphi_1(\bar{p},0)\dot{\varphi}_2(\bar{p},0) - \varphi_2(\bar{p},0)\dot{\varphi}_1(\bar{p},0)} +$$

$$+C(\bar{p},z_0)\varphi_2(\bar{p},z_0) ,$$

$$\dot{\varphi}_2(\bar{p},z) = \frac{\partial\varphi_2(\bar{p},z)}{\partial z} , \quad \vartheta(x) = \begin{cases} 1 & x\geq 0 \\ 0 & x<0 \end{cases} .$$

Functions $\varphi_1(p,z)$, $\varphi_2(p,z)$ are linearly independent solutions of equation

$$\frac{\partial^2}{\partial z^2}f(z,\bar{p}) + \left(\frac{\omega^2}{c(z)} - |\bar{p}|^2\right)\cdot f(z,\bar{p})=0 \qquad (2.3.3)$$

and $\varphi_2(H,\bar{p})\cdot Z_H(H) + \dot{\varphi}_2(H,\bar{p}) = 0$.

Using conditions U_I I U_{II}

$$U_I\big|_{z=h}=U_{II}\big|_{z=h} , \quad \frac{\partial U_I}{\partial z}\bigg|_{z=h} = \frac{\partial U_{II}}{\partial z}\bigg|_{z=h} \qquad (2.3.4)$$

one can obtain the next expression for the field U_I:

$$U_I(\bar{r},z;\bar{r}_0,z_0)=\int \frac{d^2p}{(2\pi)^2}\cdot e^{i(\bar{p},\bar{r}-\bar{r}_0)}\cdot\frac{e^{i\kappa(h-z)}\varphi_2(\bar{p},z_0)}{\dot{\varphi}_2(\bar{p},h)+i\kappa\varphi_2(\bar{p},h}+$$

(2.3.5)

$$+\int \frac{d^2p}{(2\pi)^2}\cdot e^{i(\bar{p},\bar{r})}\cdot\frac{e^{i\kappa z}-V_h(p)e^{-i\kappa z}}{2i\kappa}\cdot V(\bar{p}|\bar{r}_0,z_0)\ ,$$

where coefficient

$$V_h(\bar{p})=\frac{\dot{\varphi}_2(\bar{p},h)-i\kappa\varphi_2(\bar{p},h)}{\dot{\varphi}_2(\bar{p},h)+i\kappa\varphi_2(\bar{p},h)}\cdot e^{2i\kappa h}\ .$$

It is followed from (2.3.5) that $V(\bar{p}|\bar{r}_0,z_0)$ satisfies to stochastic integral equation:

$$V(\bar{p}|\bar{r}_0,z_0)=\int \frac{d^2p}{(2\pi)^2}\cdot e^{-i(\bar{p},\bar{r}_0)-i\kappa h}\cdot\frac{\varphi_2(\bar{p},z_0)}{\dot{\varphi}_2(\bar{p},h)+i\kappa\varphi_2(\bar{p},h)}b_+(\bar{q},\bar{p}|\mu(\bar{r}))+$$

(2.3.6)

$$+\int \frac{d^2p}{(2\pi)^2}\,\frac{b_-(\bar{q},\bar{p}|\mu(\bar{r}))-V_h(\bar{p})b_+(\bar{q},\bar{p}|\mu(\bar{r}))}{2i\kappa}\cdot V(\bar{p}|\bar{r}_0,z_0)$$

where

$$b_{\pm}(\bar{q},\bar{p}|\mu(\bar{r}))=\int d^2r\int dz\cdot e^{-i(\bar{q}-\bar{p},\bar{r})}\cdot\delta(z-\mu(\bar{r}))\cdot\Big[-Z_0(z)+i\kappa-$$

$$-(\bar{q},\bar{\nabla}\mu(\bar{r}))\Big]\cdot e^{-i(\kappa_1\pm\kappa)z}\ ,$$

$$\kappa_1 = \sqrt{\frac{\omega^2}{c_0^2} - |\bar{q}|^2}$$

To obtain the equation for the mean scattering field we have to average (2.3.6) over $\mu(\bar{r})$. The assumption that repeated reflections of sound field from ice cover are uncorrelated allows to present correlators $< b_{\pm}(\bar{q},\bar{p}|_{\mu(\bar{r})})\ V(p|\bar{r}_0,z_0) >$ as production $<b_{\pm}(\bar{q},\bar{p}|_{\mu(\bar{r})})>\ <V(\bar{p}|\bar{r}_0,z_0')>$. In this case average integral equation has a solution

$$<V(\bar{q}|\bar{r}_0,z_0)> = \frac{\varphi_2(\bar{q},\bar{r}_0)e^{-i\kappa_1 h - i(\bar{q},\bar{r}_0)}}{\varphi_2(\bar{q},h)+i\kappa_1\varphi_2(\bar{q},h)} \cdot \frac{2i\kappa_1 Q_+(\kappa_1)}{2i\kappa_1 - Q_-(\kappa_1)+V_h(\bar{q})Q_+(\kappa_1)} \tag{2.3.7}$$

where

$$Q_{\pm}(\kappa) = Q_{\pm}(\kappa,\kappa_1)\Big|_{\kappa=\kappa_1},$$

$$Q_{\pm}(\kappa,\kappa_1) = -Z_{\sigma}(\kappa\pm\kappa_1) + i\kappa\cdot e^{-1/2\sigma^2(\kappa\pm\kappa_1)^2},$$

$$Z_{\sigma}(\kappa\pm\kappa_1)=\frac{1}{\sigma\sqrt{2\pi}}\cdot\int_{-\infty}^{+\infty} dv\cdot Z_0(v)\cdot e^{-\frac{v^2}{2\sigma^2} - iv(\kappa\pm\kappa_1)}.$$

Let us average expressions (2.3.4), (2.3.5) and take the limit $h\Rightarrow 0$. Then we may write boundary conditions for the averaged scattering field <U> at z=0 with effective impedance K which takes into account the scattering properties of the rough boundary. Presenting field <U> as Fourier transform

$$\langle U(\bar{r},z;\bar{r}_0,z_0)\rangle=\int\frac{d^2p}{(2\pi)^2}\cdot e^{i(\bar{p},\bar{r}-\bar{r}_0)}\cdot g(z,z_0,\bar{p}) \tag{2.3.8}$$

one can obtain boundary condition at z=0

$$\dot{g}(0,z_0,\bar{p}) = - K(\bar{p})\cdot g(0,z_0,\bar{p}) .$$

where

$$K(\bar{p})=i\kappa\cdot\frac{2i\kappa - Q_-(\kappa) - Q_+(\kappa)}{2i\kappa - Q_-(\kappa) + Q_+(\kappa)} \tag{2.3.9}$$

It is follows from (2.3.2), (2.3.3), (2.3.8) that mean sound field

$$\langle U(\bar{r},z;\bar{r}_0,z_0)\rangle =$$

$$=\int\frac{d^2p}{(2\pi)^2}e^{i(\bar{p},\bar{r}-\bar{r}_0)}\frac{\psi_1(\bar{p},z)\psi_2(\bar{p},z_0)\vartheta(z_0-z) + \psi_1(\bar{p},z_0)\psi_2(\bar{p},z)\vartheta(z-z_0)}{\psi_1(\bar{p},\ 0)\dot{\psi}_2(\bar{p},\ 0) - \psi_2(\bar{p},\ 0)\dot{\psi}_1(\bar{p},\ 0)} \tag{2.3.10}$$

where $\psi_1(\bar{p},z)$, $\psi_2(\bar{p},z)$ satisfy to equation (2.3.3) and boundary conditions

$$\dot{\psi}_1(\bar{p},0) = - K(\bar{p})\cdot\psi_1(\bar{p},0), \tag{2.3.11}$$

$$\dot{\psi}_2(\bar{p},H) = Z_H(H)\cdot\psi_2(\bar{p},H) \tag{2.3.12}$$

Using (2.3.10), (2.3.11), (2.3.12) one can consider situations when assumption that repeated reflections are uncorrelated does not hold. In these cases effective impedance K is expressed by series which is similar in simplest series of renormalization theory in quantum field theory where the first nontrivial approximation is uncorrelated repeated reflections approximation. Notice that used

approach to solution of the problem of scattering by statistical rough boundary allows to obtain analytical expression for the second statistical moment of scattered field. The expression (2.3.10) is wave representation for the mean field and incorporates both ray approximation and mode one.

In calculations of detection zones and localization of sources of high frequency signals at small ranges the simplest variant of the ray representation (three rays representation) is used. Sound field <U> is presented as

$$<U(\bar{r},z;\ \bar{r}_0,z_0)>\sim \sum_{j=1}^{3} A_j(\bar{r},z;\bar{r}_0,z_0)\cdot e^{iS_j(\bar{r},z;\bar{r}_0,z_0)} \qquad (2.3.13)$$

where the first term describes the field of the water ray, second term describes the field of the ray reflected from ice cover and second term describes the field of the ray reflected from the bottom. The coefficient of reflection from ice is approximated by expression (see 2.3.1)

$$V = V_0\cdot e^{-2\kappa^2\sigma^2},$$

where V_0 is the coefficient of reflection from smooth ice. This expression may be obtained by the boundary condition (2.3.11). To do that we have to take Ψ_1 in WKB - approximation and to assume that impedance $Z_0(r)$ is little varied in the scale of order σ. Representation (2.3.13) is justified at the range of order of the length of ray cycle which comes to the receiver. If the source and the receiver are placed in the near-surface part of the waveguide then the length of the ray cycle is approximately equal to 4 km. At the middle range multirays representation (j>3) is used. In the similar calculations for low frequency signals mode representation of sound field is used

$$\langle U(\bar{r},z;\bar{r}_0,z_0)\rangle = \sum_m A_m(|\bar{r}-\bar{r}_0|)\cdot\Phi_m(z,z_0) \qquad (2.3.14)$$

where

$$A_m(|\bar{r}-\bar{r}_0|)=\frac{2\pi i\lambda_m H_0^{(1)}(\lambda_m|\bar{r}-\bar{r}_0|)}{\dot{\psi}_1(\lambda_m,0)\left[\frac{\partial}{\partial\bar{p}}Q(\bar{p})\right]\Big|_{|\bar{p}|=\lambda_m}}, \qquad (2.3.15)$$

$$Q(\bar{p}) = \dot{\psi}_2(\bar{p},0) + K(\bar{p})\cdot\psi_2(\bar{p},0) ,$$

$$Q(\lambda_m) = 0 ,$$

$$\Phi_m(z,z_0)=\psi_1(\lambda_m,z)\cdot\psi_2(\lambda_m,z_0)\cdot\vartheta(z_0-z)+\psi_1(\lambda_m,z_0)\cdot\psi_2(\lambda_m,z)\cdot\vartheta(zz_0).$$

However the possibilities of our computers are limited so we have to consider the situation when low frequency signal propagates under ice free water. The work is continued toward the construction of the effective mode programs for calculation of the sound field under ice cover in approximation of noncorrelated reflections. At the next stages we shall enter into consideration of the second statistical moment of the sound field and estimate influence of scattering field on the efficiency of the detection algorithms.

2.4. The characteristics of ambient noise in the Eastern Arctic.

The noise of sea covered with ice is significantly different from the sea noise for the ice free water a for it is generated by another sources. The primary sources of noise generation are the impacts of floating ice which are due to stream, wind and fracturing of ice generated by the interior stresses in the course of high

diurnal overfalls of temperature in atmosphere. At period of high winds the noise is generated by movement of snow along the rough external ice surface and by turbulent vorticity of the wind. Close to melting icebergs the noise is initiated by release of air bubbles which are frozen in the body of iceberg [12]. Reviews of previously done works concerning the ice noise are presented in [17-19]. Beginning with 1970, a number of the papers on the ice noise is continued to grow. We mention papers which deal with given region only. The noise of pack ice was studied in the Fram IV expedition [20] in the neighborhood of the point 83^0 N, 20^0 E in April 1982 . The ambient noise was investigated as well in experiment CEAREX [22] in October 1988 in the same region approximately. The analysis of the spring noise was carried out in [14]. The noise registered in [22] was used to check the model of the prime causes of noise generation in the considered area [15].

According to [14] the noise is characterized by the properties as follows. It is nonstationary with respect to time. In particular the RMS of noise in the frequency range 10 ÷ 20 Hz during some days may be changed fivefold and more. The interval of the autocorrelation of changes of RMS value at the level of 0.5 is approximately 1 day. The spectrum of these changes is decreasing function of frequency. At the frequency interval from 0.1 to 10 cycles per day the corresponding "decreasing" account for 3 orders of magnitude when the velocity is approximated by $(f)^{-1.5}$. The discrete component corresponding diurnal frequency and connected with of night fall of temperature is pronounced weakly as well as the discrete component at semidiurnal frequency due to flows. The changes of RMS values of noise with respect to time are well correlated with changes of longitudinal Koriolis force and with the forces which are due to wind and water currents. The coefficient of correlation is approximately 0.7 - 0.8. The local data relative to the flows and the wind is connected with the region having linear size of order of hundred kilometers (up to 1000 km). It is this region where the basic sources of noise for of frequency range

(10 - 20 Hz) are situated . The strong changes of the noise level with semidiurnal period was noticed in [22] (as differentiated from [14]).

The changes of order of 20 dB were observed for 1/3 octave band with the mean frequencies of order of tens Hz. Such periods of noise level change in other regions reported in a number of papers (see for example [13]).

The spectral characteristics of the ice noise must be considered for concrete conditions in connection with noise nonstationarity. The spectrum of noise which have been registered in the expedition of the Acoustics Institute carried out during 1988 - 1989 for the deep water region of the Arctic is presented in Fig.2.4.1. The corresponding levels are given in dB relatively 10^{-6} Pa/$\sqrt{\text{Hz}}$. Dashed curves correspond to the conditions of the far hummocking, solid curves are for conditions of the near hummocking. Three pairs of curves correspond to the noise levels which are not exceeded the fixed level with probabilities: 0.1, 0.5 and 0.9. The comparison of these curves with spectrum in [14] demonstrates that the data of Fram IV correspond to the probability 0.9 at the condition of the shut-range hummocking. When the ice displacements is small both the far and the near hummocking are absent and the noise level is essentially reduced. The low-frequency spectrum had been obtained for such conditions in the same expedition and presented in Fig.2.4.2. Here the figures denote the probability of unexceedness of given level. It is seen that the curves are placed 7 - 10 dB below than that corresponding to Fig.2.4.1.

The noise level depends on season. On the average the level is a several dB greater in winter than in summer. In spring the probability of noise occurrence is increased as a result of fracturing of ice caused by the abrupt changes of temperature when passing from midnoon to night and vice versa [10]. In this case the generated sound pulse looks like damped sinusoidal signal. The central frequency and the coefficient of attenuation are depended on the size of ice-floe [16]. The spectrum of signal occupies the frequency band from some tens to some thousands Hz.

If the fracturing are produced from many ice-floes then the pulses are overlapped and the distribution of total signal may be approximated by the normal distribution. Otherwise the deviations from the normal law are possible [8]. Usually, the deviations from normal distribution are observed under the high frequencies and at small depths . These deviations can be characterized by excess coefficient which is equal to zero when the deviations are absent. According to [11] this coefficient reaches value 100 when the fast reduction of the temperature of air, occurs.

If the long-range hummocking are observed at all azimuthal angles then the noise is isotropic and the interval of horizontal correlation (which is evaluated as the distance to the first zero of correlation function) is approximately one-half of wavelength. Under the short-range hummocking the isotropy is impaired and the intervals of horizontal correlation are in creased [9].

The bearing of sounds produced by the cracking of the short-range ice-floes may be taken with high accuracy by rays which are not reflected from ice. The intervals of signals correlation associated with reflected rays may be calculated by the programs taking into account the roughness of lower surface of ice. The vertical interval of correlation is determined by the range of noise arrival angles.

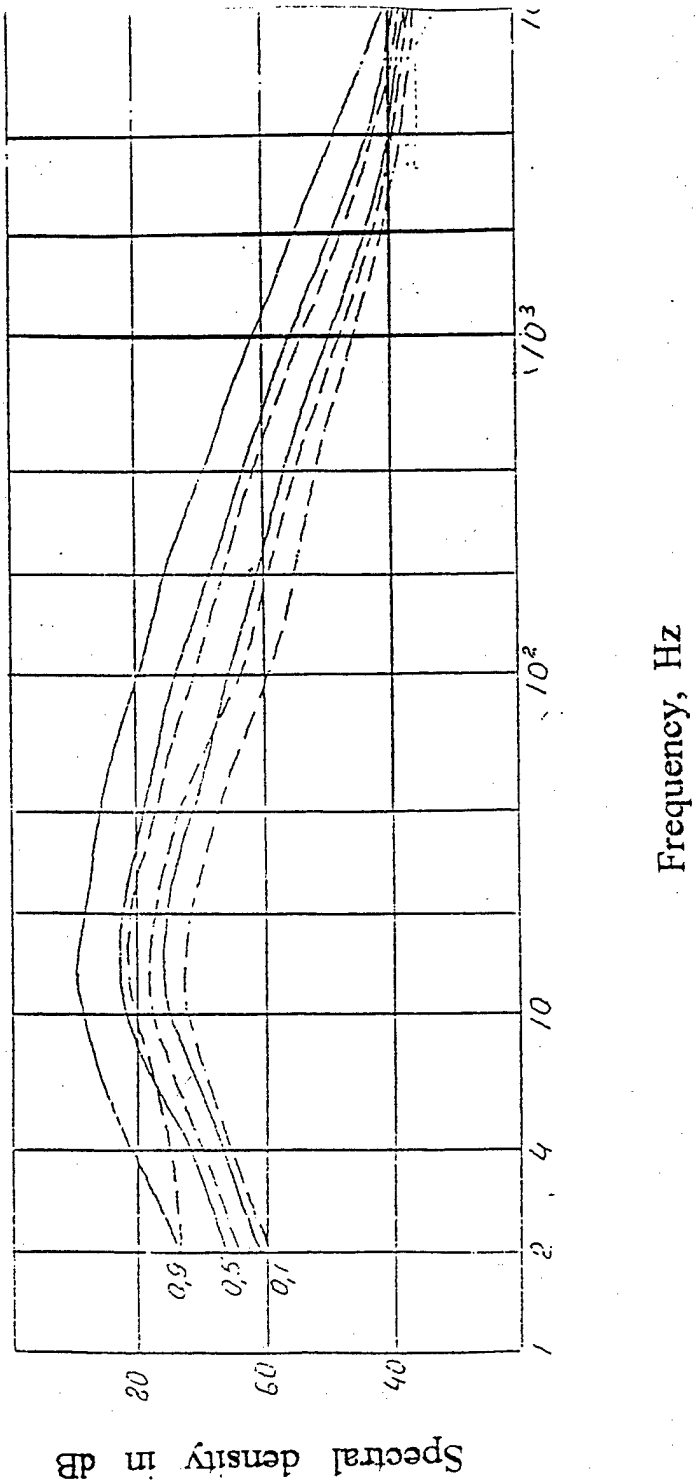

Fig. 2.4.1. Spectrum of the under ice noise in the deep water region of the Arctic. The solid line indicates the conditions of the near hummocking. The dashed line indicates the conditions of the far hummocking. The numerals indicate the probability of nonexceeding of the given level.

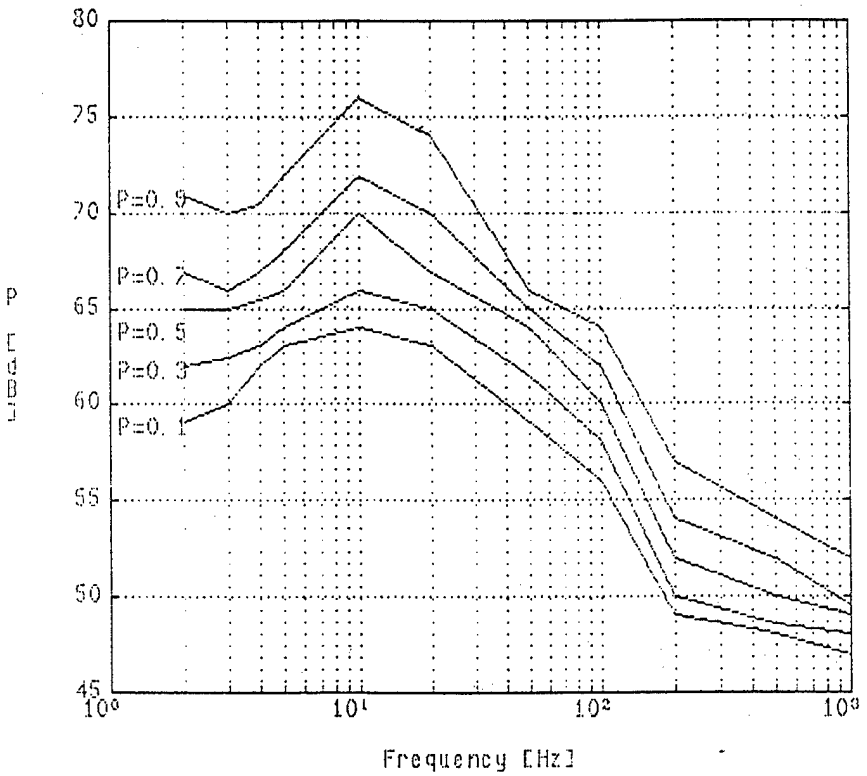

Fig. 2.4.2. Noise spectra when there is no hummocking.
Numbers are the probabilities of not excess of
the given level.

3. THE PRELIMINARY ANALYSIS OF THE VARIANTS OF THE PASSIVE SUMMM.

3.1. General considerations.

The algorithms of spatial-time processing of the SUMMM must solve the following tasks: detection, localization with the estimation of the parameters of MM movement trajectories and identification of the detected MM. This is a traditional approach and we will follow it further.

The construction of effective detection, localization and trajectory analysis algorithms can be done using modern methods of theoretical statistics and theory of signal processing taking into account the peculiarities of the tasks to be solved. We hope to extend detailed analysis of the algorithms and their modifications for our case at following stages of this project using principles of maximum likelihood, optimal filtration and etc. In actual conditions algorithms are valid when ambiguity with respect to signals and noises statistical characteristics takes place. This requires the application of adaptation and invariance principles. For example, the use of Neuman-Pearson concept for the solution of detection problem in the conditions of unknown noise parameters requires the false alarm stabilization and hence the application of these principles. Here we limit ourselves by the analysis of the simple processing algorithms, which in turn allow to get simple technical realization. The exception is the long-range SUMMM where the ideas and principles of matched field processing are used.

In our situation the task of identification is very complicated problem. It is connected above all with absence of sufficient body of the experimental data which makes possible construction of the models for the solution of the identification task. In the conditions of such fuzzy description of the models, the creation of effective classification rule is rather problematic. Therefore it is necessary to use

common efforts both biologists and signal processing experts for creation of the models and the identification algorithms at the following stages of the project.

3.2. The SUMMM for detection, localization and telemetry with use of tags .

In this paragraph we consider the key characteristics of the SUMMM with three types of signals: tone-pulse signals, pseudonoise-pulse signals and large BT signals.

3.2.1. Spatial-frequency characteristics of a source.

It is assumed in the calculations that the radiation and the reception are omnidirectional ones. This circumstance is important when the energetic optimal frequency range is looked for. It should be noted that the concept of optimal frequency in hydrolocation is similar one for the underwater communication [18]

The attenuation of the sound in the water is determined by the formula (see sec. 2)

$$\beta(f) = b \cdot f^{\alpha} \qquad \text{dB/km} \tag{3.2.1}$$

The spectrai density of ambient isotropic noise (dynamic sea noise) can be determined by

$$P^2_{n0}(f) = B_n \cdot f^{-n} \qquad \text{Pa}^2/\text{Hz}, \tag{3.2.2}$$

It follows from (3.2.2) that the optimal frequency is

$$f_{opt} = \left(\frac{n}{0.23\ \alpha br} \right)^{1/\alpha} \qquad \text{kHz}, \tag{3.2.3}$$

where distance red by kilometers.

Taking

$$b = 0.025,$$
$$\alpha = 1.5, \qquad (3.2.4)$$
$$n = 1.68,$$

we obtain

$$f_{opt1} = 33.6 \text{ kHz} \qquad \text{at } r = 1 \text{ km}, \qquad (3.2.5)$$

and

$$f_{opt2} = 21.2 \text{ kHz} \qquad \text{at } r = 2 \text{ km}.$$

As it was noted in section 2.1 the choice of operating frequency range should be done taking into account the adverse influence of the radiation on marine mammals as well. From this point of view the frequency (3.2.5) is low. It should be increased according to notice in section 1.

This brings up the question: How many energetic losses are taken place when the operating frequency deviate from the optimal one. The simple mathematical transformations lead to the following ratio of expression for corresponding SNR:

$$\frac{q^2(f)}{q^2(f_{opt})} = f^n \cdot \left(0.626 \frac{\alpha b r}{n} \right)^{n/\alpha} \exp\left(-0.23 b f^{\alpha} r \right). \qquad (3.2.6)$$

Substituting values of the parameters from (3.2.4) into (3.2.6) we obtain.

$$10 \lg \frac{q^2(f)}{q^2(f_{opt})} =$$

$$= -0.025f^{1.5} \cdot r + 16.8 \lg f + 1.12 \lg r - 20.8 \quad \text{dB.} \tag{3.2.7}$$

If for example the energetic losses in the SUMMM is of order of 3 dB then according to (3.2.7) the mean frequency of the operating range is

$$f_{m_1} = 60 \text{ kHz} \qquad \text{at } r = 1 \text{ km},$$

$$f_{m_2} = 40 \text{ kHz} \qquad \text{at } r = 2 \text{ km}. \tag{3.2.8}$$

The simple electroacoustic transducers with omnidirectional radiation have the relative frequency band of order of 10 % [32].

Thus the operating frequency range of the SUMMM is in actual practice limited by the band

$$\Delta f_1 = 6 \text{ kHz} \qquad \text{at } r = 1 \text{ km},$$

$$\Delta f_2 = 4 \text{ kHz} \qquad \text{at } r = 2 \text{ km}, \tag{3.2.9}$$

with values of mean frequency to be equal 60 kHz and 40 kHz according to (3.2.8).

3.2.2. The characteristics of the SUMMM with ton-pulse signals.

In accordance with (2.1.2) if the resolution capacity of range measurements is Δr = 10m then the duration of ton-pulse signal should be equal

$$\tau_t \simeq 6.67 \cdot 10^{-3} \text{ sec} \tag{3.2.10}$$

The period of ton-pulse repetition is chosen as

$$T_S = 2 \text{ sec} \tag{3.2.11}$$

(setting $T_S = \Delta r/V_{MM}$ and $V_{MM} = 5$ m/sec. In this case on-off time $Q_t = T_S/\tau_t \cong 300$).

Let us assume that the receiver can be realized by the procedure of noncoherent detection of one ray signal. In this case the probability of false alarm (PFA) and the detection probability (PD) can be evaluated by the below formula from reference [33] (optimistic case)

$$q^2_{\varphi d} \approx \left(\sqrt{\ln \frac{1}{PFA}} + \sqrt{\ln \frac{1}{PLS} - 1.4} \right)^2. \tag{3.2.12}$$

where PLS=1-PD and $q^2_{\varphi d}$ is the ratio of the signal energy to spectral density of additive white noise at the input of the receiver.

Taking

$$PFA_d = 10^{-3},$$

$$PLS_d = 10^{-1}, \tag{3.2.13}$$

we obtain the required signal/noise ratio

$$q^2_{\varphi d} = 12.8 \longrightarrow 11 \text{ dB}. \tag{3.2.14}$$

If the signal detection is done for obtaining the information then the requirements for the probability of error are more severe

$$PFA_i = PLS_i = 10^{-3}. \tag{3.2.15}$$

Then

$$q^2_{\varphi d} = 24.8 \longrightarrow 14 \text{ dB}. \tag{3.2.16}$$

When the Rayleigh fading take place caused for example by multiray sound propagation (pessimistic case) the threshold SNR may be evaluated by [33]:

$$q^2_f \approx \frac{1}{PLS} \ln\frac{1}{PFA}, \tag{3.2.17}$$

and in accordance with (3.2.13), (3.2.15) we obtain

$$q_{fd} = 69 \longrightarrow 18 \text{ dB},$$

$$q_{fd} = 6900 \longrightarrow 38 \text{ dB}. \tag{3.2.18}$$

Let us evaluate the number of MM which can be separated by the considering SUMMM. The frequency shift ΔF_t of signals for the MM identification must be done taking into account the possible Doppler shift, that is

$$\Delta F_t = F_t + 2\Delta F_d. \tag{3.2.19}$$

Taking into account (3.2.8) we can write

$$\Delta F_{d1} \frac{V_b}{c} \cdot f_{m1} \approx 200 \text{ Hz} \quad (r=1\text{km}),$$

$$\Delta F_{\alpha 2} \frac{V_b}{c} \cdot f_{m2} \approx 135 \text{ Hz} \quad (r=2\text{km}). \tag{3.2.20}$$

As

$$F_t = \frac{1}{\tau_t} = 150 \quad \text{Hz}, \tag{3.2.21}$$

then we obtain

$$\Delta F_{t1} = 550 \text{ Hz},$$

$$\Delta F_{t2} = 420 \text{ Hz}. \tag{3.2.22}$$

The number of the frequency shifted signals which can be formed using the frequency band Δf is

$$N_t = \frac{\Delta f}{\Delta F_t}. \tag{3.2.23}$$

Thus taking into account (3.2.9) and (3.2.22) we obtain

$$N_{t1} = 11,$$

$$N_{t2} = 9. \tag{3.2.24}$$

This means that using such SUMMM allows to identify sufficiently large number of MM.

In accordance with 2.1 the SUMMM with ton-pulse signals can be used for transmission of information. For example, in the system with the operating range r =2km one of N_{t2} =9 frequency channels can be used for the positioning of MM and as an synchronization channel under transmission of binary information by the rest of eight partial frequency channels. In this case the source has to radiate up to 9 frequency-shifted signals simultaneously. The consumption of energy is increased as much as 4 times approximately. The speed of information transmission (for the single MM) in the given variant is

$$R_t = \frac{(N_t-1)}{T_s} \quad \frac{bit}{sec}. \tag{3.2.25}$$

At T_s=2 sec

$$R_{t1} = 5 \quad \frac{bit}{sec}, \tag{3.2.26}$$

$$R_{t2} = 4 \quad \frac{bit}{sec}.$$

Let us make an estimate the parameters of MM which can be transmitted in this case.

(i) For the transmission of pulse rate it is sufficiently to transmit about 7 bit of information (128 gradation) per minute. Here the speed of transmission of the information is about 0.1 bit/sec.

(ii) For transmission of temperature from one point of MM's body it is sufficient to use 9 bit (512 gradation) for the measurement of absolute values of temperature with an accuracy of 0.1^0. Under the sampling of data of temperature sensor with the interval of 1 min the speed of transmission is 0.15 bit/sec. Thus the temperature can be measured from several points of MM's body.

Thus due to the SUMMM with the localization and the measurement of the physiological parameters of MM can be performed for several MM by tone-pulse signals.

3.2.3. The characteristics of the SUMMM with pseudonoise-pulse signals.

In accordance with (3.1) in the SUMMM with pseudonoise-pulse signals the pulses duration τ_n and the period of their repetition T_s are remained as before, that is

$$\tau_n = \tau_t \approx 6.67 \cdot 10^{-3} \text{ sec}, \tag{3.2.27}$$

$$T_s = 2 \text{ sec}.$$

However the band of radiated signal is increased

$$F_{n1} = 10\Delta F_{d1} = 2000 \text{ Hz} \qquad (r = 1 \text{ km}),$$
$$F_{n2} = 10\Delta F_{d2} = 1350 \text{ Hz} \qquad (r = 2 \text{ km}). \tag{3.2.28}$$

The product of the frequency band of signal and its duration is

$$B_{n1} = \tau_n \cdot F_{n1} \approx 13,$$
$$B_{n2} = \tau_n \cdot F_{n2} \approx 9. \tag{3.2.29}$$

This system do not requires the Doppler correction of receiving signal.

The evaluation of the performance of a receiver of the SUMMM with pseudonoise-pulse signals with parameters (3.2.29) for actual hydroacoustic channel is a hard problem. However it should be noted that the signal with parameters (3.2.29) is less subjected to the influence of the fading by interference than ton-pulse signals. Therefore evaluated levels of radiation in this system will be closer to the optimistic levels then to the pessimistic ones.

The number of possible frequency shifted signals is determined by

$$N_n = \frac{\Delta f}{F_n}. \tag{3.2.30}$$

Taking into account (3.2.9), (3.2.28) we obtain

$$N_{n1} = N_{n2} = 3, \tag{3.2.31}$$

This is noticeably less than in (3.2.24) but is quite workable from practical point

of view.

In using the system of the N_n frequency shifted pseudonoise - pulse signals for simultaneous positioning and telemetry of single MM the speed of information transmission is determined as in (3.2.25) and equal to

$$R_{n1} = R_{n2} = 1 \qquad \text{bit/sec.} \tag{3.2.32}$$

As it is follows from (i), (ii) (the sec. 3.2.2) this speed provides the telemetry of the main physiological parameters of MM.

3.2.4. The SUMMM characteristics with large BT signals.

The acoustic system of underwater surveillance can be constructed as the system of the transmission of telemetric information and of trajectory measurements of MM by an array. To obtain the information about several MM simultaneously such system has to operate in accordance with principle of Random-Access Discrete-Address System [5]. In general the signals are subjected in the SUMMM to the distortions which are changed both in space and time. Therefore the system of information transmission should be constructed by the use of principles of adaptation to conditions of signal propagation [4, 34].

To increase the resolution capacity of the system the signal with maximal frequency band which is equal to bandpass of the radiating tract (3.2.9) must be used. The resolution capacity for delay ΔT and range Δr is

$$\Delta T_1 = 1/\Delta f_1 \approx 0.167 \cdot 10^{-3} \text{ sec},$$

$$\Delta T_2 = 1/\Delta f_2 \approx 0.25 \cdot 10^{-3} \text{ sec},$$

and

$$\Delta r_1 = c \cdot \Delta T_1 = 0.25 \text{ m},$$

$$\Delta r_2 = c \cdot \Delta T_2 = 0.375 \text{ m}.$$

To use the merit of large BT signals the parameter $\Delta T \Delta f$ (base of signal B) should be much more than 1. However increasing of the base B over specific limits leads to the complication of the transmitter as well as signal processing algorithms. If we limit ourselves by value [4, 34]

$$B = 1024, \tag{3.2.34}$$

then the duration of signal is

$$\tau_{B1} = \frac{1024}{\Delta f_1} = 0.17 \text{ sec} \qquad (r = 1 \text{ km}),$$

$$\tau_{B2} = \frac{1024}{\Delta f_2} = 0.256 \text{ sec} \qquad (r = 2 \text{ km}). \tag{3.2.35}$$

These signals can be transmitted currently one after another and this will allow presumably to reduce the influence of the radiation on MM. Wide band of such signals (see (3.2.9)) and its pseudonoise character is favored for the decreasing of the influence as well. For the large BT signals with period (3.2.11) the on-off time ratio is distinguished from Q_t and is equal to

$$Q_{B1} = \frac{T_S}{\tau_{B1}} \approx 11.7,$$

$$Q_{B2} = \frac{T_S}{\tau_{B2}} \approx 7.8. \tag{3.2.36}$$

The needed level of the input signal-noise ratio q_B^2 on the receiver can be evaluated by the experimental data presented in [34]. In actual conditions of multirays sound propagation of the error probabilities (3.2.15) in an adaptive receiver with signal base equal as in (3.2.24) was attained under

$$q_B^2 \approx 0.25 \longrightarrow -6 \text{ dB}. \qquad (3.2.37)$$

The ensemble of the quasiorthogonal signals is in routine used for the transmission of the information in the system with the large BT-signals. The "volume of the ensemble" is equal to the base of signal B. Consequently the speed of the transmission of the information for the current transmission of signals is equal to

$$R_{B1} = \frac{\ln B}{(\ln 2)\cdot\tau_{B1}} \approx 60 \text{ bit/sec},$$

$$R_{B2} = \frac{\ln B}{(\ln 2)\cdot\tau_{B2}} \approx 40 \text{ bit/sec}. \qquad (3.2.38)$$

In the case of transmission of signals with on-off time ratio determined by (3.2.36), the speed of transmission is decreased by a factor equal to the value of on-off time ratio.

The number of the different MM which can be identified by the system with the use of the large BT-signals is equal to the number of different M-sequences which can be produced under the given base of the signal B. It is known that if B=1023, then

$$N_B = 60. \qquad (3.2.39)$$

Therefore the SUMMM with the large BT-signals allows to realize sufficiently large possibilities from point of view of reliable operating of the SUMMM both for the solution of the localization problem and for the information transmission in multiray conditions of sound propagation.

3.3. The SUMMM with the use of marine mammal signals.

In this section we concentrate our attention on the variant of the low-frequency SUMMM with a large operating range.

Let us assume that the system operates as follows. The problem of detection

and localization of MM is solved during relatively short time interval. The estimate trajectory of MM is constructed as the result of sequential measurements of coordinates due to the appropriate smoothing procedure for example, due to Kalmen-Bucy procedure or its modifications.

Sure this is suboptimal procedure as compared with the procedures of detection and estimation of trajectory as whole. However this is simple procedure and we will base on the one further.

As a first approximation, let us assume that the movement of MM is not effected of the system operation at single interval of observation. This assumption follows from the relation between velocities of the movement of MM, the size of the array and the range to MM (more detailed analysis is possible at the next stage of the project).

Using the frequency representation of observed by corresponding normalized FT signals the observation on the array can be presented by

$$\bar{z}(f)=\eta(f)\,\bar{H}(f,\bar{r})+\bar{\xi}(f),\quad f\in F, \qquad (3.3.1)$$

where $\bar{z}(f)$ is the vector of observations at the array at the frequency f, $\eta(f)$ is radiated signal of the point source, $\bar{H}(f)$ - is the vector determined by Green function which describes the sound propagation from the point $\bar{r}$ to the array and $\bar{\xi}(f)$ is the vector of noise. F is the set of frequencies which are multiplex $\frac{1}{T}$ in the band of frequency analysis (T is the observation time). In this case $\bar{z}(f)$, $f\in F$, is approximately defined as the consequence of independent random complex vectors with mean $\eta(f)\ \bar{H}(f)$ and correlation matrix $G_{\xi}(f)=M\{\bar{\xi}(f)\ \bar{\xi}^{+}(f)\}$. The symbol $M\{\cdot\}$ denotes the operation of mathematical expectation, + - the operation of transposition and of

conjugation.

Let us consider several variants of the detection problem.

(i) The model of stochastic signal. By determining spectral density of signal $g_S(f)=M|\eta(f)|^2$ we obtain the following expression for likelihood ratio:

$$L(\bar{Z}_F) = \sum_{f\in F}\left[-\ln(1+g_S(f)\ \Gamma(f)) + \frac{g_S(f)\ |U(f)|^2}{1+g_S(f)\ \Gamma(f)} \right] \tag{3.3.2}$$

where

$$\Gamma(f)=\bar{H}^{+}(f)\ G_{\xi}^{-1}(f)\ \bar{H}(f)$$

$$U(f)=\bar{H}^{-+}(f)\ G_{\xi}^{-1}(f)\ \bar{z}(f) \tag{3.3.3}$$

Using the local optimality principle the following expression for the detection statistics can be obtained:

$$T(\bar{Z}_F)=\sum_{f\in F} g_S(f)|U(f)|^2 \tag{3.3.4}$$

Notice that

$$M_0\{U(f)\}=0;\quad D_0\{U(f)\}=\bar{H}^{-+}(f)\ G_{\xi}^{-1}(f)\bar{H}(f)=\Gamma(f)$$

$$M_1\{U(f)\}=0;\qquad D_1\{U(f)\}= \tag{3.3.5}$$

$$=\bar{H}^{+}(f)\ G_{\xi}^{-1}(f)\ \bar{H}(f) + \tilde{g}_S(f)\left|\tilde{\bar{H}}^{+}(f)\ G_{\xi}^{-1}(f)\bar{H}(f)\right|^2$$

where $\tilde{g}_S(f)$ is "true" values of signal spectral density and $\tilde{\bar{H}}(f)$ - the vector which

determines the sound propagation in the medium. The "mismatching" between $\bar{H}(f)$ and $\tilde{\simeq}$ $H(f)$ can be caused for example by "focusing" of the array to the point different from the source point, by incorrect specification of the waveguide parameters and etc..

The calculation of the distribution of statistics $T(\bar{Z}_F)$ under the hypothesis H_0 (the signal is absent) and under alternative H_1 (the signal is present) is nontrivial problem. The needed programs were in actual developed. However the powerful computer is required in order to make application of the SUMMM-PAC useful.

Therefore we consider here two variants: $T \cdot \Delta f >> 1$ and $T \cdot \Delta f \simeq 1$ where T is the observation time and Δf is the frequency band of the signal. In the first case it is possible to use gaussian approximation (due to the first term of Edgeworth expansion) for the distribution function of $T(\bar{Z}_F)$. The probability of correct detection PD for weak signal in determined by

$$PD = 1 - \Phi\ (A_{1-\alpha} - q) \tag{3.3.6}$$

where

PFA=α (PFA is false alarm probability), $A_{1-\alpha} = \Phi^{-1}(1-\alpha)$ $\Phi(x) = \frac{1}{\sqrt{2\pi}} \int_{-\infty}^{x} \exp\{ - t^2/2\}dt$

and

$$q = \frac{\sum_{f \in F} g_s(f)\tilde{g}_s(f)|\tilde{\simeq}H^{+}(f)G_{\xi}^{-1}(f)\bar{H}(f)|^2}{(\sum_{f \in F} g_s^2(f)(\bar{H}^{+}(f)G_{\xi}^{-1}(f)\bar{H}(f)^2)^{1/2}}$$

In the second case

$$PD = \alpha^{\frac{1}{1+q(f)}} \tag{2.3.7}$$

where

$$q(f) = \frac{\tilde{g}_S(f)\left|\tilde{\bar{H}}(f)G_\xi^{-1}(f)\bar{H}(f)\right|^2}{\bar{H}^+(f)G_\xi^{-1}(f)\bar{H}(f)}$$

If $g = \tilde{g}$ and $\bar{H} = \tilde{\bar{H}}$ then in the first case

$$q = \left\{\sum_{f\in F} g_S^2(f)\cdot(\bar{H}^+(f)\cdot G_\xi^{-1}(f)\cdot\bar{H}(f))^2\right\}^{1/2} \tag{3.3.8}$$

and in the second case:

$$q(f) = g_S(f)\cdot\bar{H}^+(f)\cdot G_\xi^{-1}(f)\cdot\bar{H}(f) \tag{3.3.9}$$

The calculation of the detection zones in the first version of the SUMMM-PAC is based on the use of these formula.

The simplest model of MM signals which can be used as a first approximation is the model of the harmonic signal on the observation time interval [0,T] with unknown frequency. Then dividing the operating frequency band into subbandes (of order of $\frac{1}{T}$) the detection statistics can be determined as maximal value among the outputs of spatial processing at given frequencies. In this case the approximate method of the PD evaluation is in change α by $\frac{\alpha}{m}$ where m is the number of the subbandes.

In next stages of the work it is expected that the more accurate analysis can

be carried out including the variants when the frequency is changing within observation interval and when the more complicated model of the MM signal (for example polyharmonic one) is used.

(ii) Another model of radiated signal is that the signal is unknown. This is a extreme case of course and it reflects the pessimistic viewpoint here.

When signal is known the conditional likelihood ratio is determined as:

$$L(\bar{Z}_F) = \sum_{f\in F}\left[2\mathrm{Re}\{\eta^*(f)\cdot U(f)\} - |\eta(f)|^2\cdot\Gamma(f) \right] \tag{3.3.10}$$

If the signal is unknown then the use of maximal likelihood principle give rise to the following detection statistics

$$T(\bar{Z}_F) = \sum_{f\in F} \frac{|U(f)|^2}{\Gamma(f)} \tag{3.3.11}$$

In our case:

$$M_0\{U(f)\}=0; \quad D_0\{U(f)\}=\bar{H}^+(f)\cdot G_\xi^{-1}(f)\cdot\bar{H}(f)=\Gamma(f) \tag{3.3.12}$$

$$M_1\{U(f)\}=\eta(f)\cdot\tilde{H}^+(f)\cdot G_\xi^{-1}(f)\cdot\bar{H}(f); \quad D_1\{U(f)\}=\bar{H}(f)\cdot G_\xi^{-1}(f)\cdot\bar{H}(f)=\Gamma(f)$$

It follows from (3.3.11) that the distribution of the statistics under hypothesis H_1 is the distribution of the sum of random values having noncentral κ^2 distribution.

When $T\cdot\Delta f\simeq 1$ the statistics $T(\bar{Z}_F)$ (3.3.11) under hypothesis H_0 have the noncentral κ^2 distribution. The parameter of noncentrality is

$$\frac{|\eta(f)|^2 \cdot |\tilde{\bar{H}}^{+}(f) \cdot G_{\xi}^{-1}(f) \cdot \bar{H}(f)|^2}{\bar{H}^{+}(f) \cdot G_{\xi}^{-1}(f) \cdot \bar{H}(f)};$$

For the model of monochromatic signal with unknown frequency the corresponding modifications are similar the above.

The performance of the localization procedure of MM is determined by general ambiguity function

$$\kappa(\bar{r}_1, \bar{r}_2; H, \tilde{H}; g_S, \tilde{g}_S) =$$

$$= \frac{\sum_{f \in F} g_S(f) \tilde{g}_S(f) |\tilde{\bar{H}}^{+}(f, \bar{r}_1) G_{\xi}^{-1}(f) \bar{H}(f, \bar{r}_2)|^2}{\left(\sum_{f \in F} \tilde{g}_S^2(f) (\tilde{\bar{H}}^{+}(f, r_1) G_{\xi}^{-1}(f) \tilde{\bar{H}}(f, \bar{r}_1))^2 \right)^{\frac{1}{2}} \left(\sum_{f \in F} g_S^2(f) (\bar{H}^{+}(f, \bar{r}_2) G_{\xi}^{-1}(f) \bar{H}(f, \bar{r}_2) \right)^{\frac{1}{2}}}$$

One of the justification for the use of such criterion may be done by Kullback-Leibler information distance for the case of weak signal.

Further we intend to carry out more rigorous analysis of localization performance including the analysis by Fisher's information matrix under large SNR and by appropriate information distances. Some details of these approaches and different examples of their application are in [35,36]. The stochastic model of Green function is of large interest in given problem when the middle - frequency and the high-frequency SUMMM are used. We have intentions to conduct the investigations in this direction on base of the results presented in review [37] and our earlier results as well.

4. THE BRIEF DESCRIPTION OF THE PROGRAM PACKAGE (SUMMM-PAC,VER. 1.0) FOR THE SUMMM DESIGN AND PERFORMANCE EVALUATION.

4.1. The main purpose and general description of the SUMMM-PAC.

We have developed the version 1.0 of the program package (SUMMM-PAC). The main aim of the SUMMM-PAC is to optimize the structure of the SUMMM and to choose the tactics of the SUMMM operating for given conditions. The package provides the interactive style of operation: the designer choose the signal-noise situation (characteristics of marine mammal's signals or characteristics of the source on the mammal's body and characteristics of the acoustic noise), the properties of medium for sound propagation (for example, sound speed profile, characteristics of attenuation, the programs simulating the signal's propagation and so on), configuration and location of the receiving array and the performance estimation for the field processing algorithms under investigation. The SUMMM-PAC gives the user wide capabilities of friendly interface, the system of help and many demo examples. The results are presented using the capabilities of computer graphics (2D and 3D pictures) and can be printed easily; the presentation of the results is clear and form of the presentation can be easily changed by the user. The SUMMM-PAC is the open system and allows to introduce modifications.

The SUMMM-PAC runs on the IBM PC AT computers with DRAM at least 1 Mb, graphical controller, such as VGA or SVGA under MS-DOS. It is necessary to have mouse for program operating.

Some calculations require computer with sufficiently powerful processor (at least 90 MHz). We use the language Borland Pascal to develop the program.

4.2. The structure of the SUMMM-PAC.

The main menu of the program SUMMM-PAC shown in fig.4.1 is a clear block model

for the SUMMM operating. The main menu consists of 17 blocks and the user can obtain the main characteristics of the SUMMM operating under various conditions using the blocks 1 - 15. The SUMMM performance can be presented as follows. The signal is radiated (marine mammal voices - block 1 or a source on marine mammal's body - block 12). Then the signal propagates in some underwater waveguide with some sound speed profile (block 2) and another medium parameters, such as ice surface characteristics, bottom properties, attenuation characteristics and etc. (block 3). The sound propagation is simulated by one of the programs for calculation of sound fields in ocean (block 13). Then the signal is received by an array of given configuration (block 4) in noise background (block 5). It is necessary to use various methods of signal processing (block 14) to obtain the results of the SUMMM performance. The user can obtain clear graphic presentation of the results of the main characteristics of the signal processing methods under the given conditions (block 6 - two-dimensional and three dimensional detection zones for given probabilities of detection and false alarm; block 15 - the ambiguity function body relatively to the marine mammal's coordinates) and the results of the computer simulation for mammal's tracking as well (block 16). The user can choose the block of the main menu or other submenu using double click of the mouse. There is an automatic interlock if the user tries to choose block or parameters incompatible with blocks or parameters chosen earlier.

By means of blocks 8 - 11 the modeling of the sound propagation and signal processing in the SUMMM is produced. If the user choose these blocks then he gets brief description of the SUMMM performance information and chosen methods of signal processing as well. This data can be changed, using information banks (block 1 - 5, 12 - 14). The user can choose the item of the bank using mouse. The banks can be changed and corrected easily, using special interface. The block 10 ("Processing") allows to introduce the data which is different from "actual" data (i.e. the simulation of unmatched processing is produced).

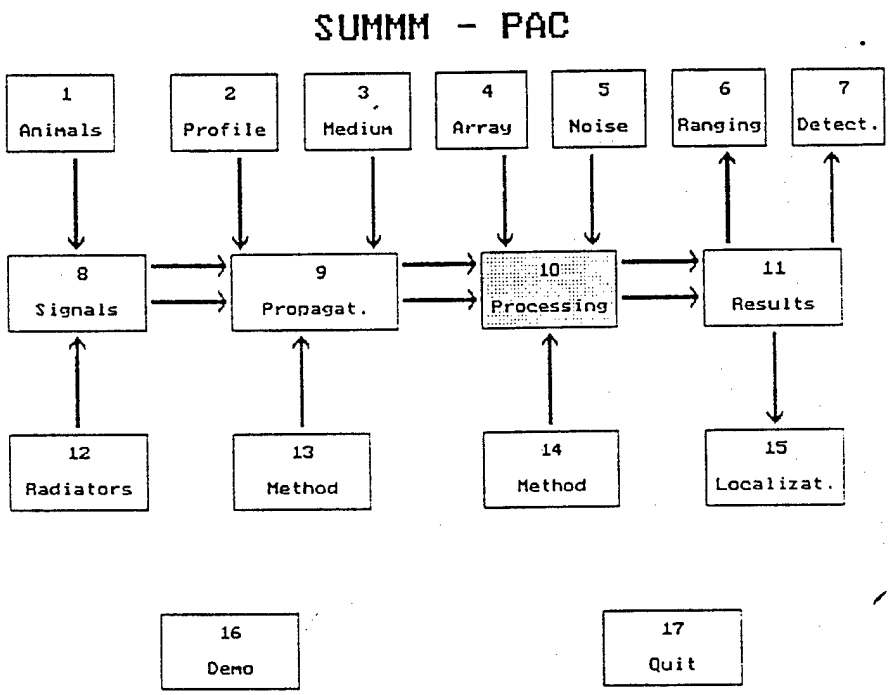

Fig. 4.1. Main menu of the program package SUMMM-PAC, version 1.0.

The information about MM is contained in block 1 (see fig.4.2).

The user chooses the type of MM and obtains the information about this species of marine mammal. One can choose the parameter of corresponding signal, frequencies, levels and etc. which are typical for the species. The information bank is supplemented continuously. It contains the results of our own research as well. There are banks contained the following information: signals from the sources attached to a mammal body (block 12), the characteristics of various underwater waveguides (blocks 2 - 3), the properties of ambient noise (block 5), are the methods of sound propagation calculation (mode and ray programs) and methods of signal processing (block 13 - 14), vertical sound speed profiles. The choice of the profile for necessary calculations is performed by mouse. The above banks admit the possibilities of correction and addition of information.

By using section "DEMO" (block 16) one can observe the demonstration of the program are demonstrated. This section comes with this report in the form of separate program.

The code is started from the file DEMO.EXE of the main directory. After the graphical title the user gets access to the main menu of the DEMO program. The program is created in turbo-vision style.

Menu item "About" contains general information about the program. The item "Main-menu" shows main menu of SUMMM-PAC. The item "Mammals" contains a part of information bank. There is also a graphic picture for the Humpback whale signal and the corresponding sonogram of this signal. One can use space bar to return to the main menu of the program or "Alt-F3" to close the text window. Item "Change-parameters" shows that a user can change parameters of MM, medium, propagation conditions, array geometry and methods of signal processing. Items "seals" and "whales" contains the results of calculations for seals and whales respectively. The

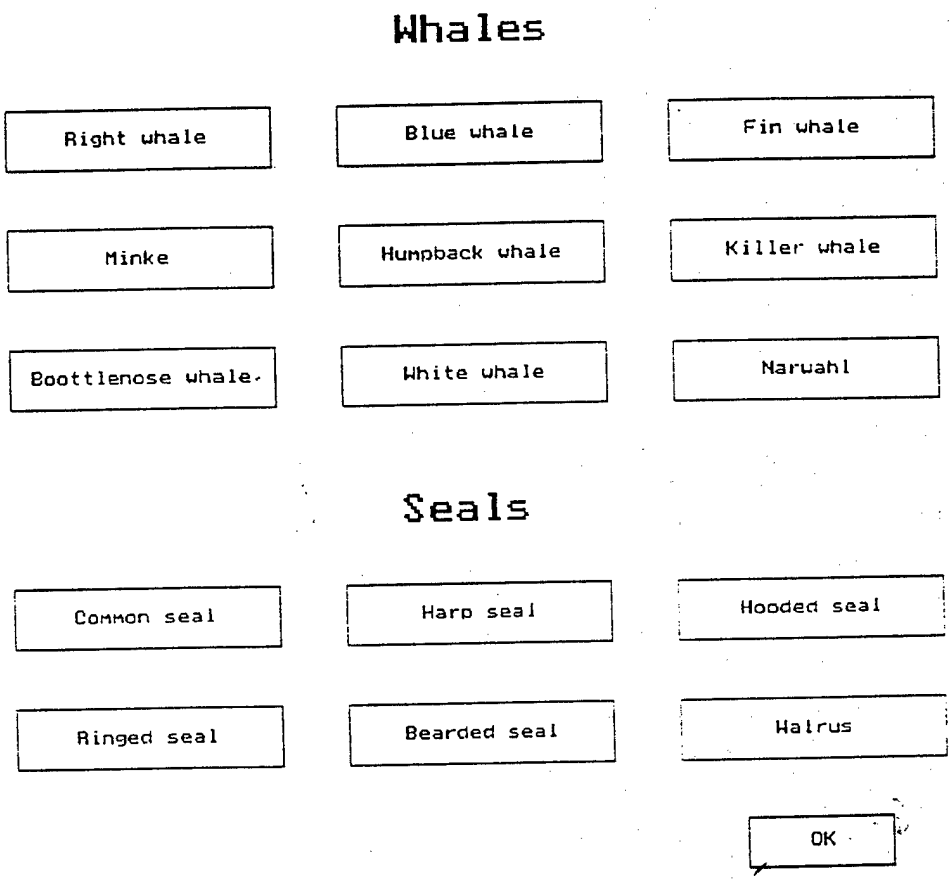

Fig. 4.2. MM information bank. Program package SUMMM-PAC, version 1.0.

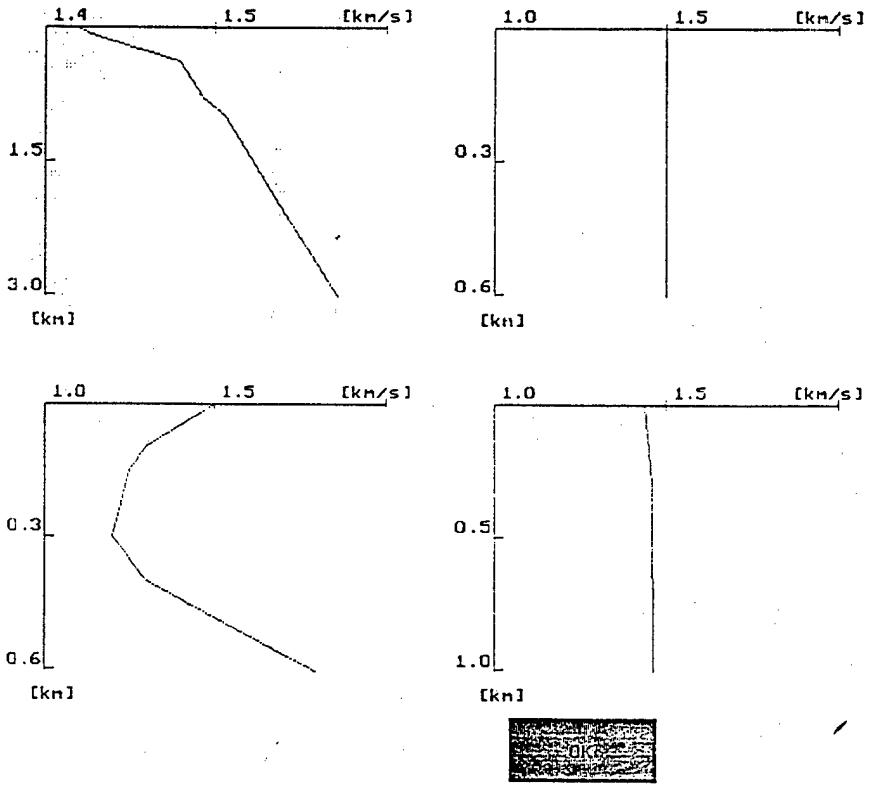

Fig. 4.3. Part of the information bank of sound speed vertical profiles. Program package SUMMM-PAC, version 1.0.

item "detection-by-horizontal-array" contains the results of the detection zones calculations for matched and unmatched field processing by horizontal array (for whales and seals).

The item "detection-by-vertical-array" shows the results of the similar calculations for the case of vertical array and contains the results of the calculations of the ambiguity function for the case of vertical array. The item "trajectories" shows the process of the MM trajectory estimation. Using the space bar allows to get the new picture or to return to main menu.

The item "Ambiguity-function-for-horizontal-array" contains the results of calculations of the ambiguity function for the case of horizontal array. The item "Ambiguity-function-for-vertical-array" contains the results of calculations of the spatial ambiguity function for the case of vertical array. The item "trajectories" shows mammal's tracking. Using the space bar allows to get the new picture or to return to main menu. Use the item "QUIT" or "Alt-X" to return from the DEMO program.

The efficiency of algorithms of MM detection and localization can be characterized by detection zones and corresponding multi-parametric ambiguity functions. The detection zone is a part of space, where detection is performed with the probability, lying in the given range when the probability of false alarm is kept fixed at some given value. The ranges of detection probability are represented by different colors of a computer monitor. The detection probabilities near 1.0 are represented by red color usually. The ambiguity function determines the change of the corresponding characteristics of detection if "true" values of corresponding parameters (for example, MM coordinates) are differed from the values used in the detection statistics. Corresponding various of ambiguity function values are represented by different colors of a computer monitor.

The formulas for the ambiguity function and detection probability calculations are presented in section 3; the examples of the calculations are presented in section

5 and are included in Demo program.

There is a computer simulation of algorithm of MM trajectory estimation with the visualization of projection of the estimation on horizontal plane. The parameters of MM movement are input in block 1 of main menu and both the trajectory and its estimation can be visualized on a computer monitor by different colors. The results of the simulation are presented in section 5 and are included in Demo program.

5. THE EXAMPLES OF THE SUMMM EFFICIENCY CALCULATIONS.

5.1. The SUMMM with tags use.

The SUMMM with tags use incorporates a device, attached to MM and intended for forming and radiating required signals. The general structural scheme of the device is shown in Fig. 5.1.1.

The device is the simplest one if the SUMMM is used only for the localization of a single or group of MM. This is pinger in Fig. 5.1.1. To obtain technical characteristics of the pinger one should continue the calculations performed in sections 3.2.2 and 3.2.3.

The results of calculations by (3.2.14), (3.2.16) and (3.2.18) allow to estimate required level of radiation. Here we have to use not only the attenuation of acoustical signals (3.2.1) but parameter B_n in (3.2.2) to be equal to

$$B_n = 1.8 \cdot 10^{-6},$$

This corresponds to data of chapter II of this volume. The required level of pressure radiated by the pinger at 1 m distance from emitter can be calculated by the formula:

$$P_{ot} = \left(2q^2 r^2 \cdot 10^6 \cdot P_{n0}^2 \cdot F_t \cdot 10^{0.1\beta(f)r} \right)^{1/2} \quad \text{Pa.} \qquad (5.1.1)$$

Here the q^2 is chosen in accordance with (3.2.14), (3.2.15) and (3.2.18), r is in km and the factor "2" shows the necessity of compensation of irregularity of emitter frequency characteristic.

Attached to MM Transmitter structural scheme

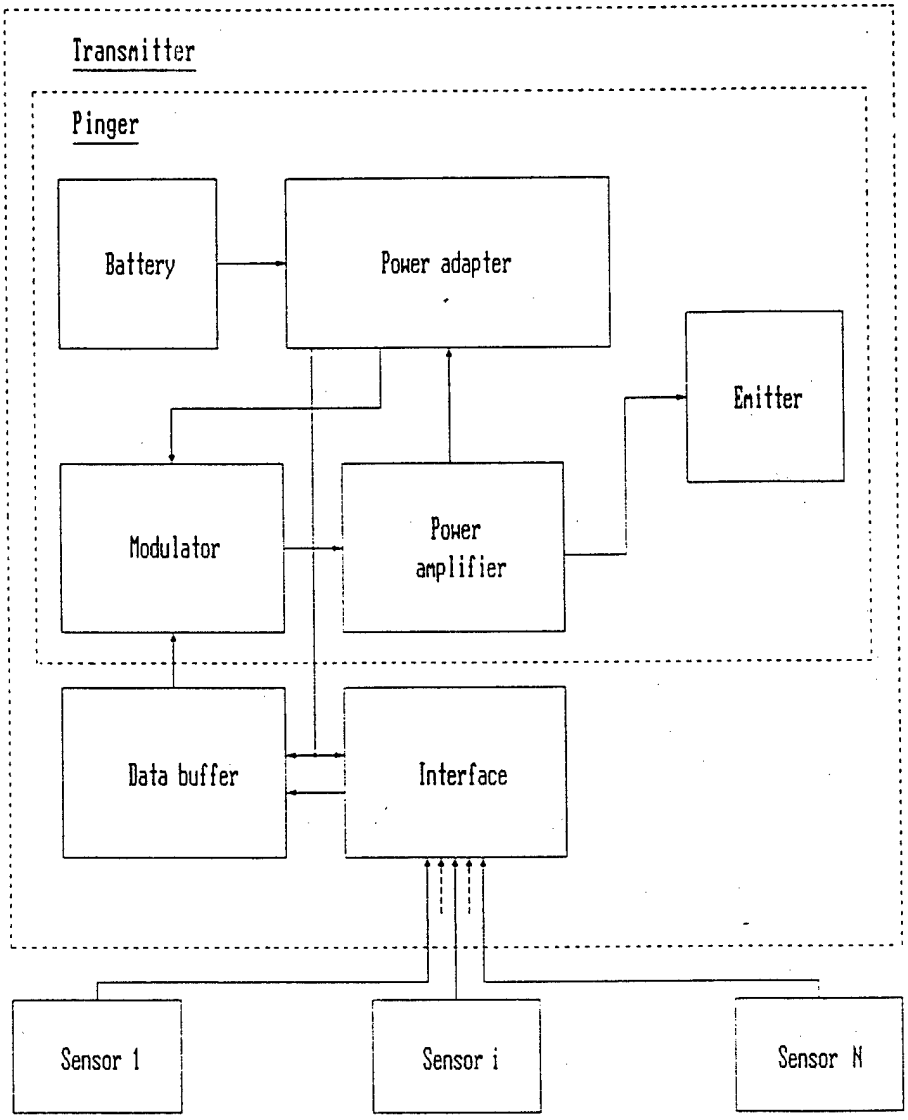

Fig. 5.1.1

The results of calculations are presented in table 5.1.1.

Table 5.1.1.

P_{ot}(Pa) in the system with ton-pulse signals

r, km	$q_{\varphi i}$ = 11 dB	$q_{\varphi i}$ = 14 dB	q_{fd} = 18 dB	q_{fi} = 38 dB
1.0	10.2	14.2	23.6	236
2.0	32.2	44.8	74.7	747

As seen from the table, in the case of Rayleigh fluctuation of the signal (see the last column) the very large levels of radiation may be required to realize the channel of telemetry.

To calculate radiated acoustical power we use the formula [32]

$$W_a = 8.4 \cdot 10^{-6} P_o^2 \qquad (5.1.2)$$

It follows from the formula that the levels of radiation less then 45 Pa correspond to the acoustical power less then 20 mW. If the efficiency of the emitter, the power amplifier and the power adapter is taken as 50 % then the estimation of consumed power is 160 mW. This corresponds to the impulse with duration τ_t or τ_n. The real consumed power of pinger Q_t is 300 times smaller.

The continuously operating schemes are the part of signals former (timer) and

power adapter. If we estimate the consumption of the timer as 0.5 mW then the average consumption of the electrical power of a pinder is obtained as

$$W_{ep} = 0.5 + 160/300 \approx 1 \quad \text{mW}. \qquad (5.1.3)$$

This is a worthwhile to use one standard airproof nikel-cadmium cell VR4 (firm SAFT) as source of electric power. It has the following characteristics:

Diameter - 32.7 mm

Height - 60.3 mm

Weight - 150 g

Voltage - 1.2 V

Capacity - 4 A•h.

Therefore the operating life of the pinger with radiation level less then 45 Pa and one cell VR4 is

$$t = \frac{4 \cdot 1.2}{1 \cdot 10^{-3}} = 4120 \text{ hours } (170 \text{ days}). \qquad (5.1.4)$$

This operating life can be increased by increasing a number of cells or using lithium batfaries.

These energetical estimations demonstrated that the realization of pinger for the SUMMM with the operating range up to 2 km when Rayleigh fluctuations of the signal take place (level 74.7 Pa from table 5.1.1) is problematic.

The sizes of the pinger can be estimated using the cell VR4 type. The cylinder has diameter 35 mm and the following lengths:60 mm for cell, 40 mm for emitter and 50 mm for electronic equipment (optimistically). Therefore, the device length is about 150 mm.

It is necessary to increase considerably radiated power and develop additional power for some additional electronic units (see Fig. 5.1.1) when the SUMMM with impulses is used for the telemetry. In this case the loss of the operating life

(5.1.4) is 5, 6 times and the increasing of the device size is approximately 50 %.

Let us consider transmitter with LBT-signals. The required level of radiated signal can be calculated using formula (5.1.1) but we have to use the frequency band (3.2.9) and don't use factor "2". The results are presented in the table 5.1.2.

Table 5.1.2.

The values of P_{OB} in the system with large BT signals

r, km	1	2
P_{OB}, Pa	6.4	16.5

The calculations of the radiated acoustical power can be done using formula (5.1.2)

$$W_{aB1} = 3.4 \cdot 10^{-4} \quad W,$$

$$W_{aB2} = 2.3 \cdot 10^{-3} \quad W. \tag{5.1.5}$$

If the efficiency of the emitter, power amplifier and power adapter is about 50% then the consumption of the electrical power can be approximately estimated as:

$$W_{eB1} = 2.7 \cdot 10^{-3} \quad W,$$

$$W_{eB2} = 18 \cdot 10^{-3} \quad W. \tag{5.1.6}$$

By analogy with way (5.1.4) we can estimate the operating life when the continuous radiation of LBT-signals takes place.

$$t_{B1} \simeq 1780 \quad \text{hours},$$

(5.1.7)

$$t_{B2} \approx 270 \quad \text{hours}.$$

If large BT signals have on-off time ratio (3.2.36) then the operating life increases. The sizes of the transmitter increases 2.0-2.5 times as compared with the pingers. The transmitter is be expected to be the cylinder with diameter 35 mm and length 300-400 mm.

5.2. The SUMMM with the use of marine mammals signals.

In this section the results of calculations and computational simulation completed by the program SUMMM-PAC for the SUMMM are presented. The viewgraphs were printed such a way that various colours of the monitor correspond to various shades of grey. The main results are presented on Fig. 5.2.1 - 5.2.13 and ones are included in Demo program. The calculations were done for two mammals: Fin whale (for the long-range SUMMM) and Harp seal (for the short-range SUMMM). The detection zones, ambiguity function cross-sections and a part of trajectory estimation for Harp seal are presented in Figures 5.2.1 - 5.2.3 respectively. The parameters of the calculations (configurations arrays, level of radiation, frequencies and etc.) are given figures legends.

As we can see from Fig. 5.2.1 operating distance for Harp seal is about 900 m if detection probability is equal to 0.8. The Fig. 5.2.2 shows that the localization accuracy of the MM is satisfactory. The efficiency of the trajectory estimation was investigated using the computional simulation. The observations were taken every 3 sec. The object moved arbitrarily with the speed to be no more then some maximum one (we use the value 5 m/sec). The trajectory estimate is the sequence of points for which the corresponding likelihood function attains maximal value. The calculations were done

using methods of optimum control for the decreasing of sorting.

There are the results of the calculations for Fin whale situated in long-range zone. Fig. 5.2.4 shows the results of simulation for Fin whale trajectory estimations (all parameters of the calculations are given under the Figure). In Fig. 5.2.5 - 5.2.6 (see Fig. 5.2.7 ÷ 5.2.8 also) horizontal cross-section of spatial ambiguity function for 4 vertical and horizontal arrays are exhibited respectively.

The detection zones of Fin whale for matched and unmatched (with respect to sound speed profile) field processing are presented in Fig. 5.2.9 and 5.2.10 respectively (when the horizontal array is used). As one can see from the figures the distance of "total detection" is about 100 km (detection probability is greater then 0.8). The matched processing have no significant advantage here. The detection probability zones for vertical array are given in Fig. 5.2.11 and 5.2.12 for matched processing and unmatched processing respectively. As one can see from figure 5.2.11 the matched processing provides the operating range for the vertical array greater then 200 km (detection probability is greater then 0.8). If one compares Figures 5.2.11 and 5.2.12 it is seen that the use of matched processing gives high advantage here. We observe ranges with the low detection probability (to be equal less then 0.4) at range 100 km from array under the unmatched processing.

The vertical cross-section of detection zones, when the detection of Fin whale is performed is presented on Figures 5.2.13 ÷ 5.2.16. Fig. 5.2.13 and 5.2.14 correspond to the case of horizontal array for unmatched and matched field processing respectively, whereas Fig. 5.2.15 and 5.2.16 are the cases for vertical array. As one can see using the vertical array gives greater range of detection then the use of the horizontal array for the case of matched processing. Besides the application of unmatched processing leads to essential loses for vertical array and a little for horizontal array.

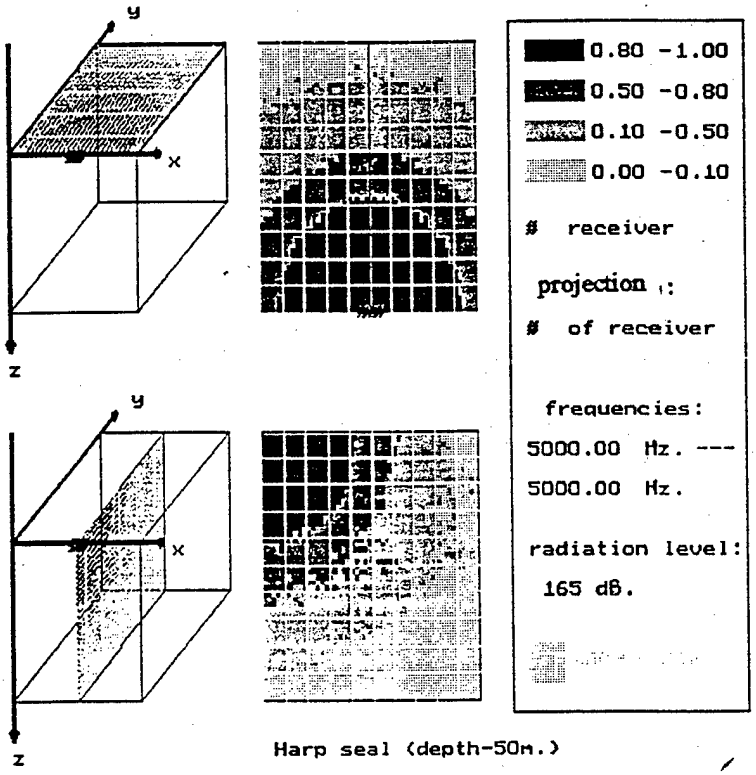

Fig. 5.2.1. Detection probability zones for Harp seal. Horizontal array, 4 receivers. Radiation level is 165 dB (relative to 1 micro- Pa at 1 m range), duration 1 sec, frequency 5 kHz. Horizontal cross-section, depth 50 m and vertical (orthogonal to base cross section), dimensions of the area: 2km x 2 km x 2 km. False alarm probability 10^{-4}.

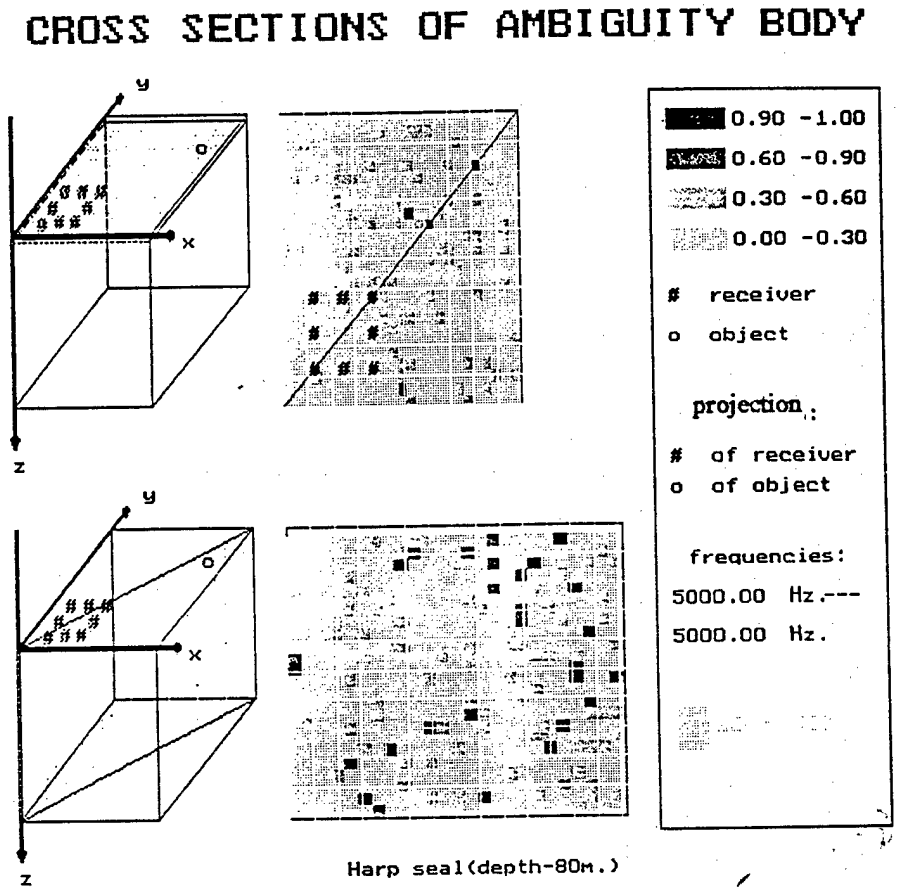

Fig. 5.2.2. Cross-section of ambiguity function body for Harp seal. Horizontal array, 8 receivers.

(see legend to Fig. 5.2.1).

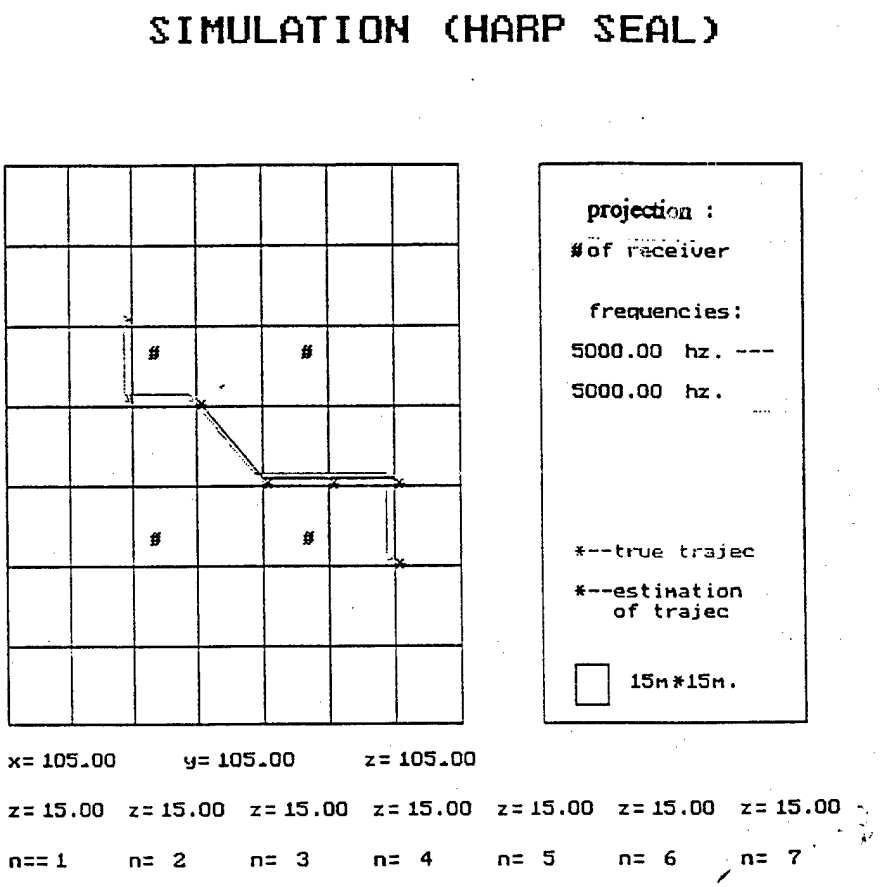

Fig. 5.2.3. Trajectory estimation of Harp seal (projection on horizontal plane). The level of signal is 145 dB. The other parameters are the same as in Fig. 5.2.1.

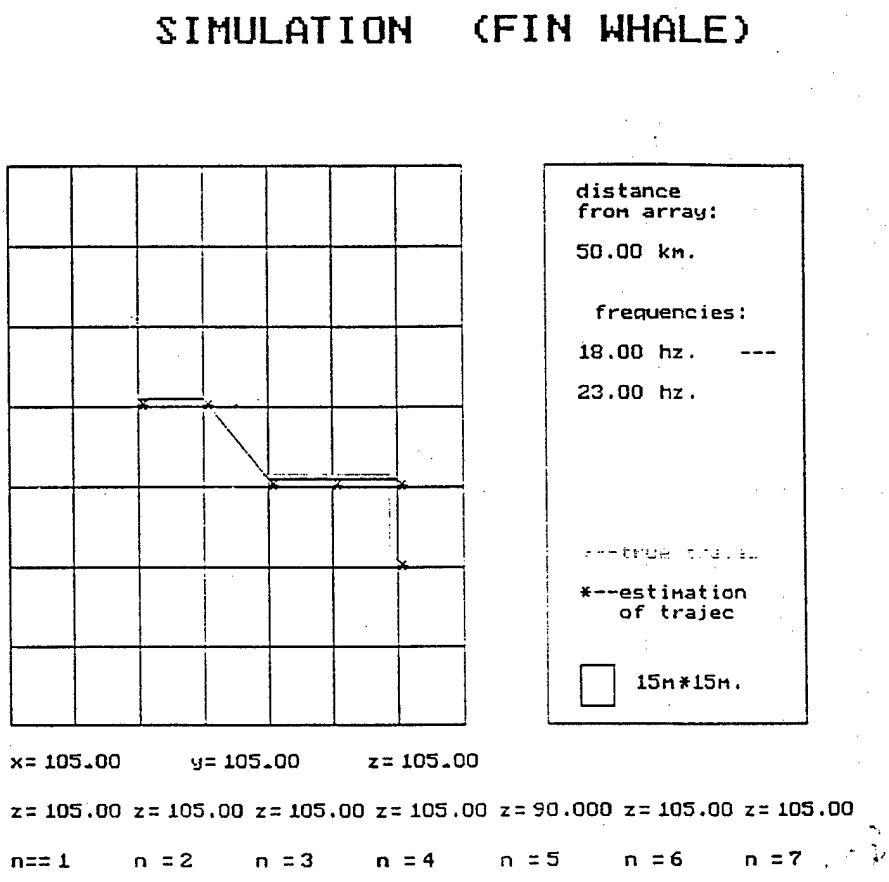

Fig. 5.2.4. Trajectory estimation for Fin whale (projection on horizontal plane). The range 50 km, level of signal 186 dB, basic frequency 20 Hz, horizontal array, 6 receivers, distance between adjacent receivers 37 m.

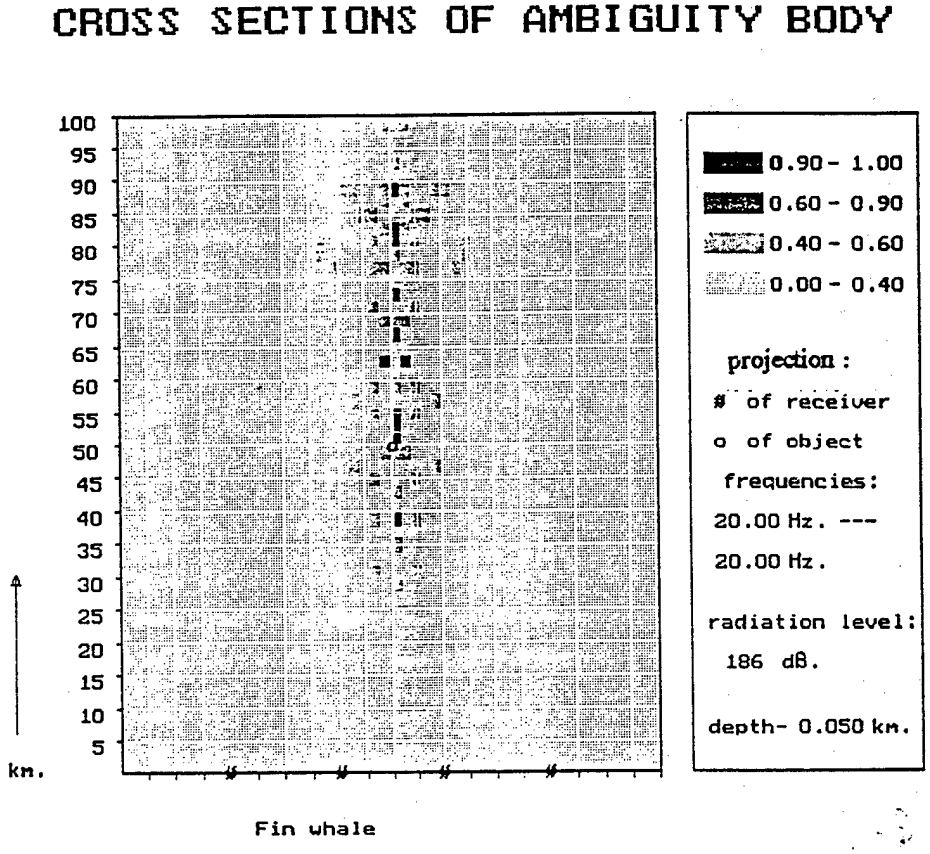

Fig. 5.2.5. Horizontal cross-sections of ambiguity function body for Fin whale, 4 horizontal arrays, 5 receivers in every array. Depth 50 m, depth of array 15 m, duration of signal 1 sec. The rest of parameters is the same as for Fig. 5.2.4.

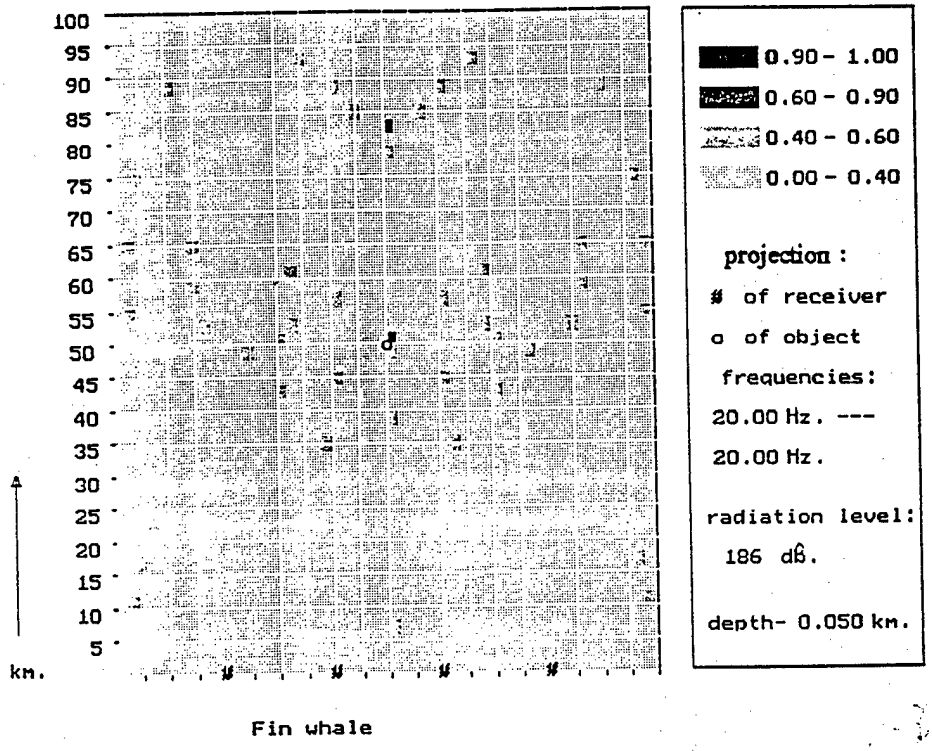

Fig. 5.2.6. 4 vertical chains, 5 receivers in every chain. The depth of upper receiver is 15 m. The rest of parameters is the same as for Fig. 5.2.5.

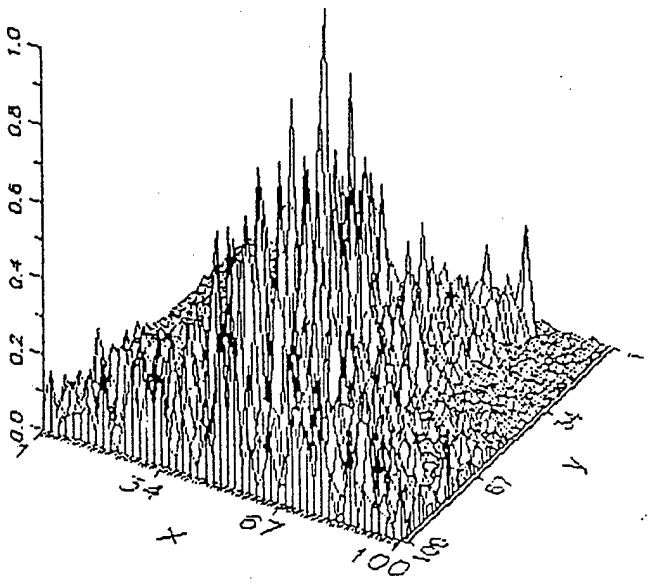

Fig. 5.2.7. Spatial ambiguity function. Parameters are the same as for Fig. 5.2.5.

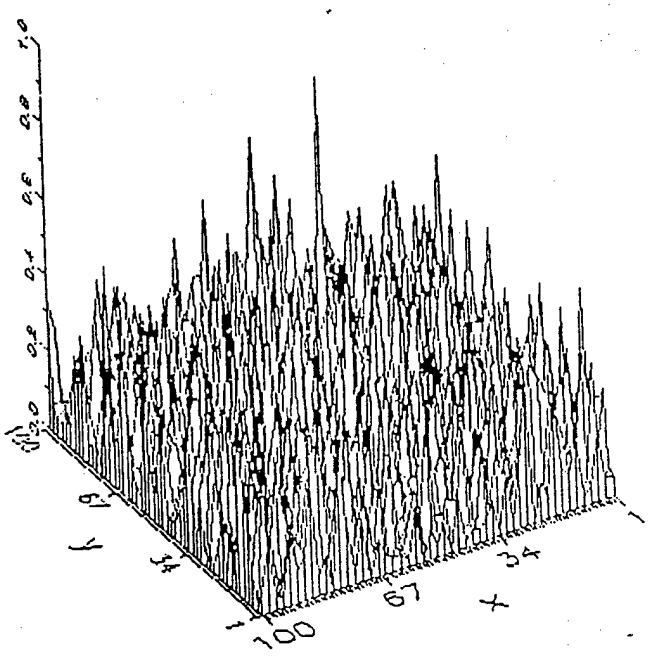

Fig. 5.2.8. Spatial ambiguity function. Parameters are the same as for Fig. 5.2.6.

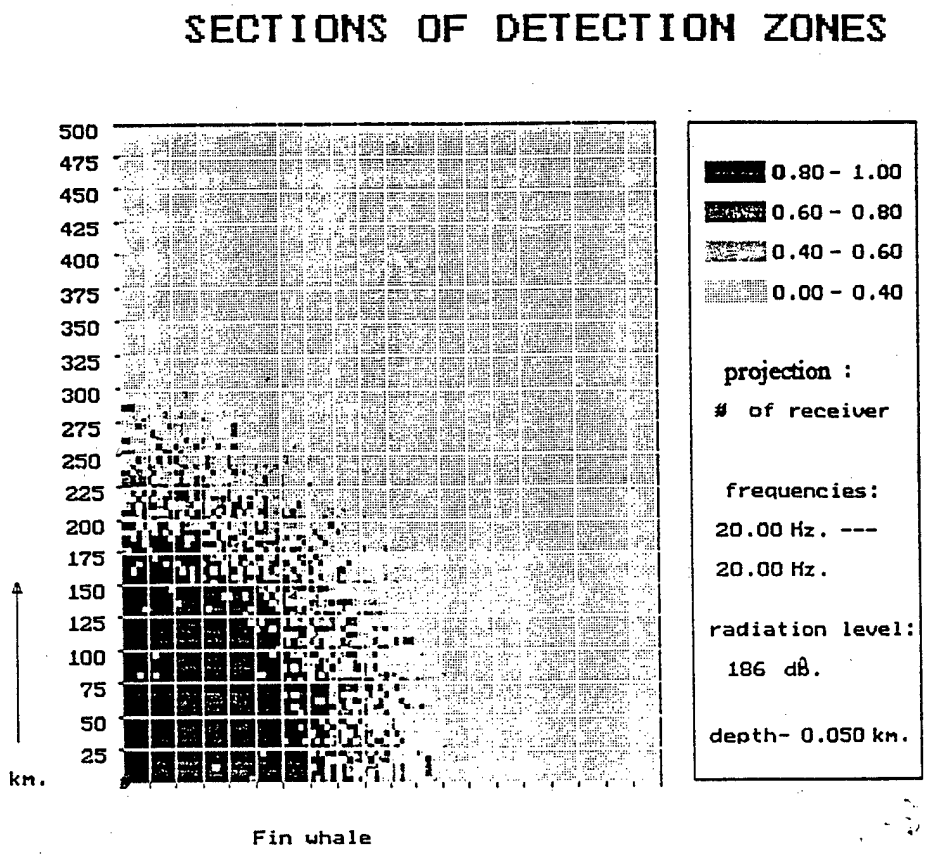

Fig. 5.2.9. Detection probability zones for Fin whale.

Horizontal array, 5 receivers, depth 15 m,

level of signal is 186 dB, basic frequency is

20 Hz duration is 1 sec; matched processing for

the speed profile corresponds to Fig. 2.3.3).

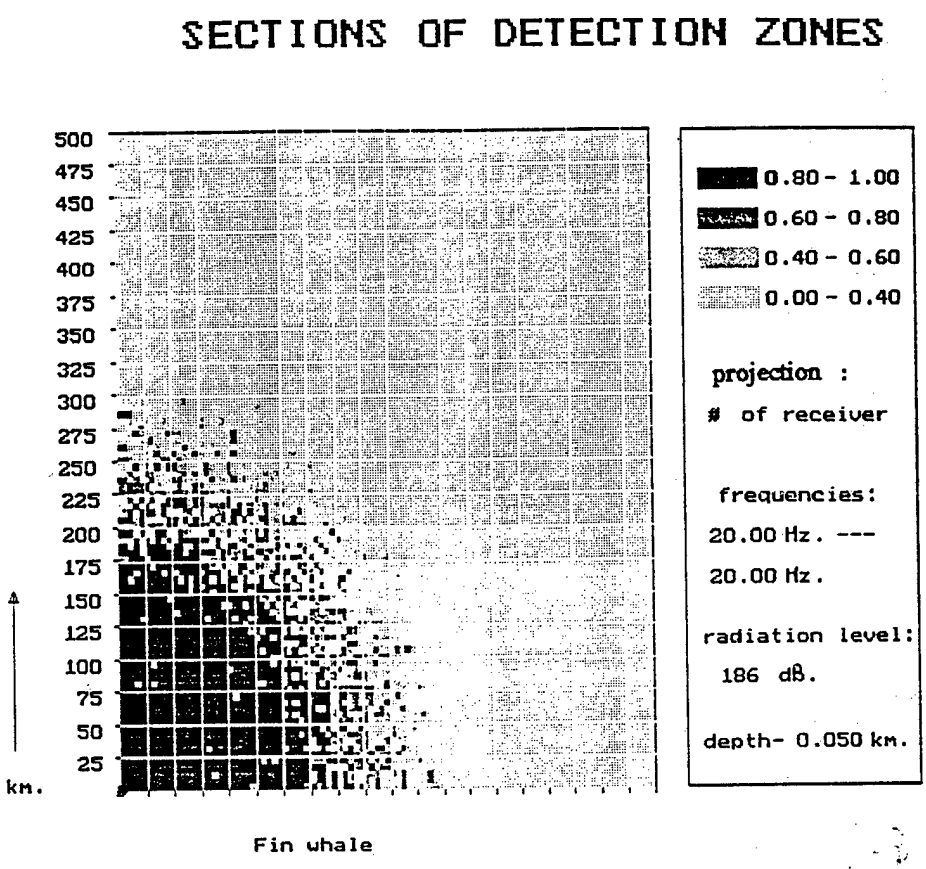

Fig. 5.2.10. Unmatched processing (see legend to Fig 5.2.9) when the isogradient speed profile is used in the detection statistics through corresponding Green's function.

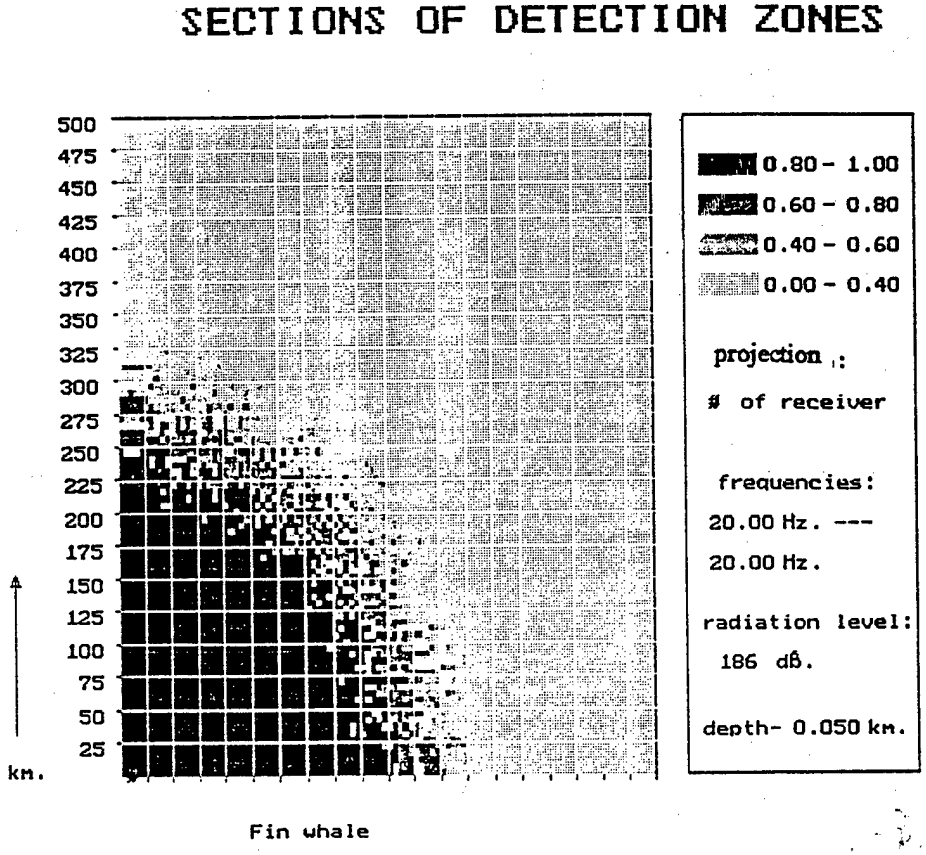

Fig. 5.2.11. Detection probability zones for Fin whale.

Vertical array, 5 receivers, depth of the upper receiver is 15 m, level of signal is 186 dB, basic frequency is 20 Hz, duration is 1 sec; match field processing.

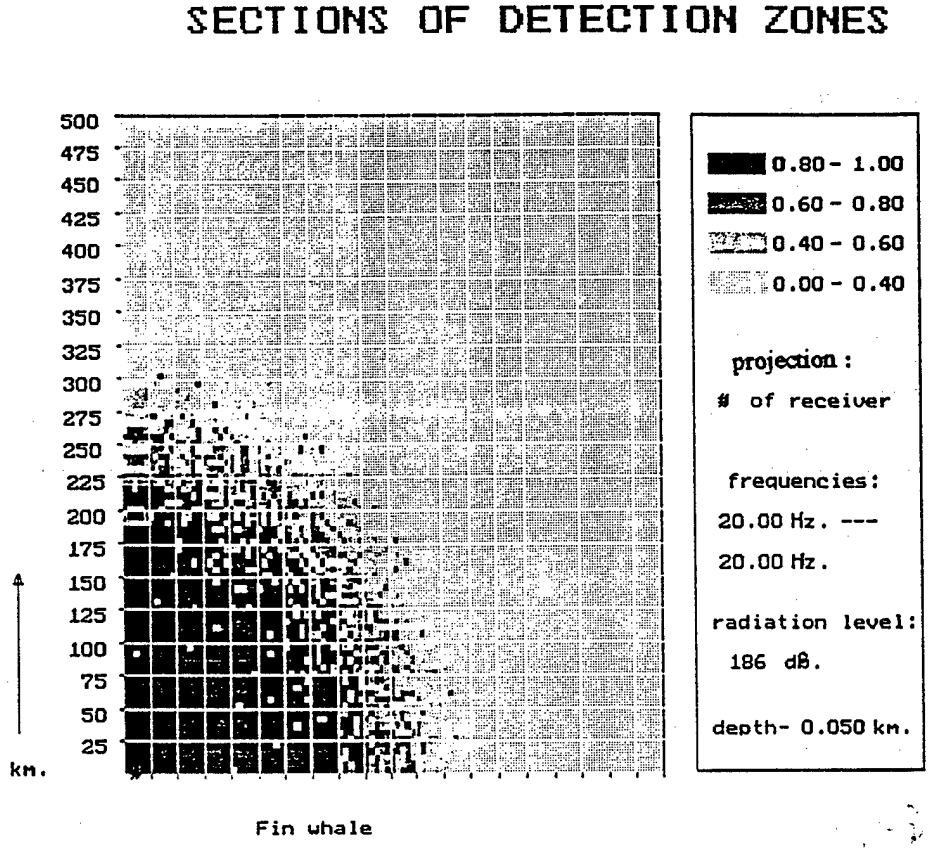

Fig. 5.2.12. Unmatched processing. Detection probability zone for Fin whale. Vertical array, 5 receiver, depth of the upper one is 15 m, signal level 186 dB, frequency 20 Hz, duration 1 sec.

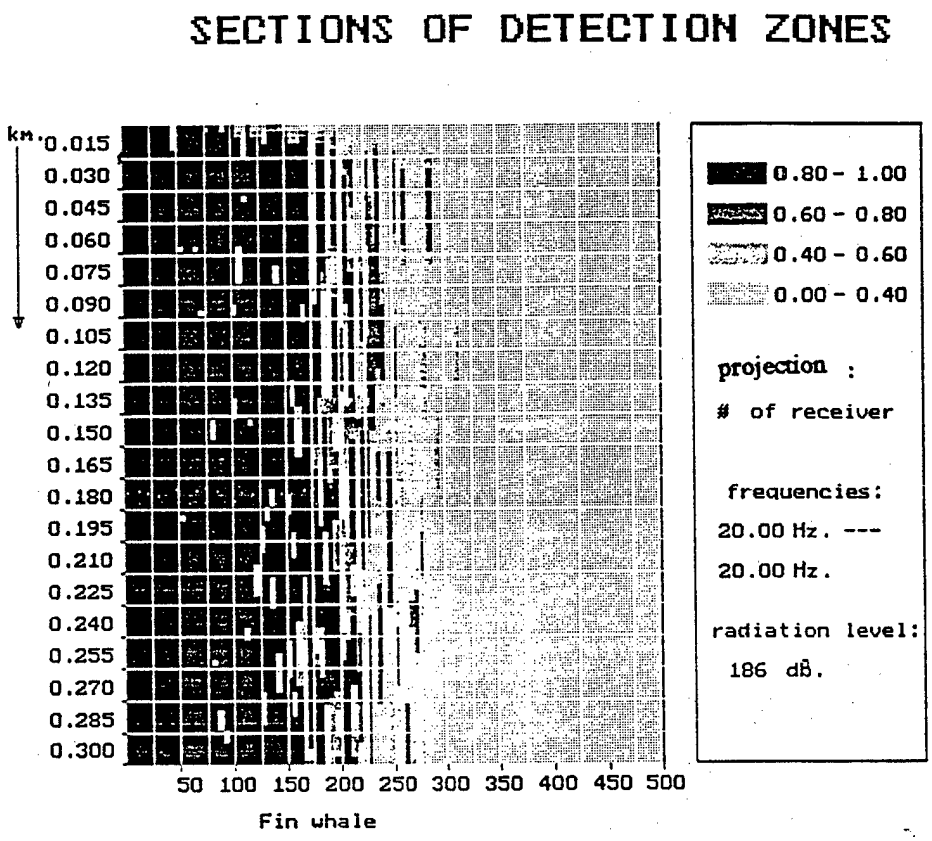

Fig. 5.2.13. Detection probability zones. Vertical cross-section, horizontal array, unmatched processing (see legend to fig. 5.2.9).

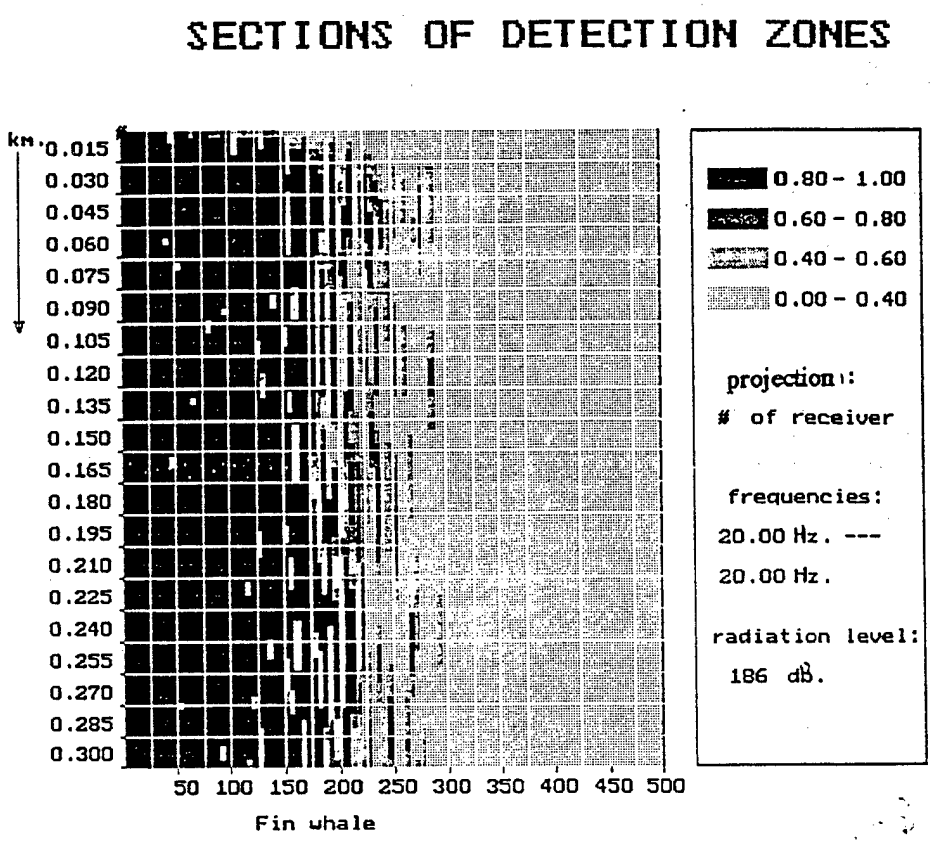

Fig. 5.2.14. Detection probability zones, vertical cross-section, horizontal array, matched processing (see legend to Fig. 5.2.9).

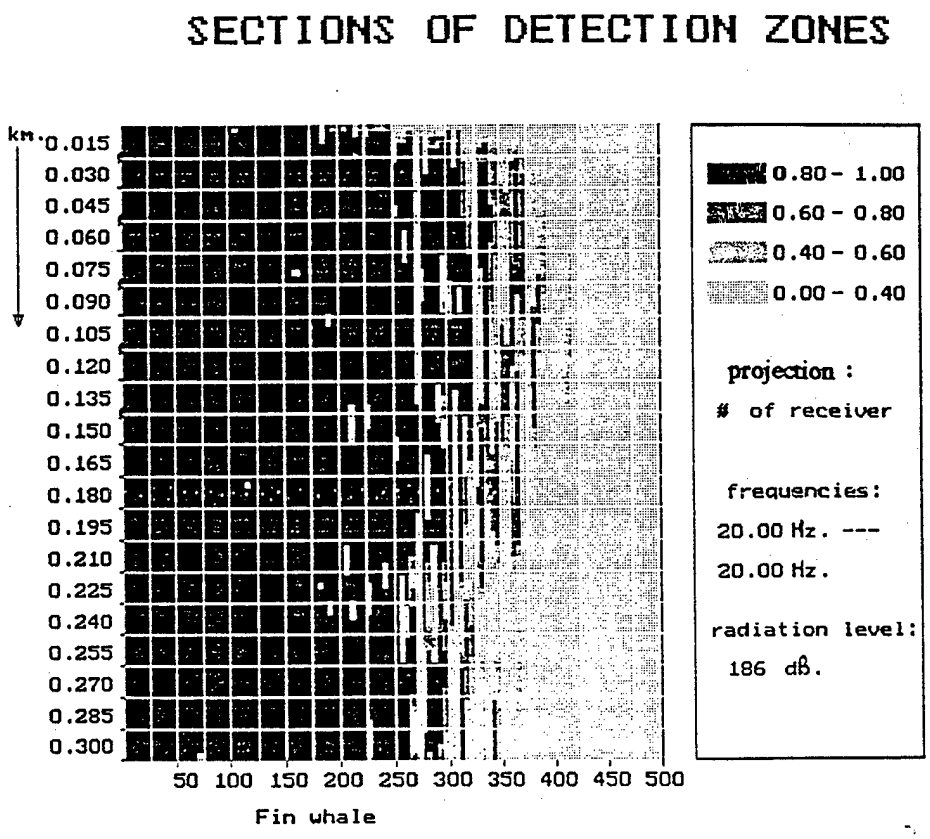

Fig. 5.2.15. Detection probability zones, vertical cross-section, a vertical array, unmatched processing (see legend to Fig. 5.2.9).

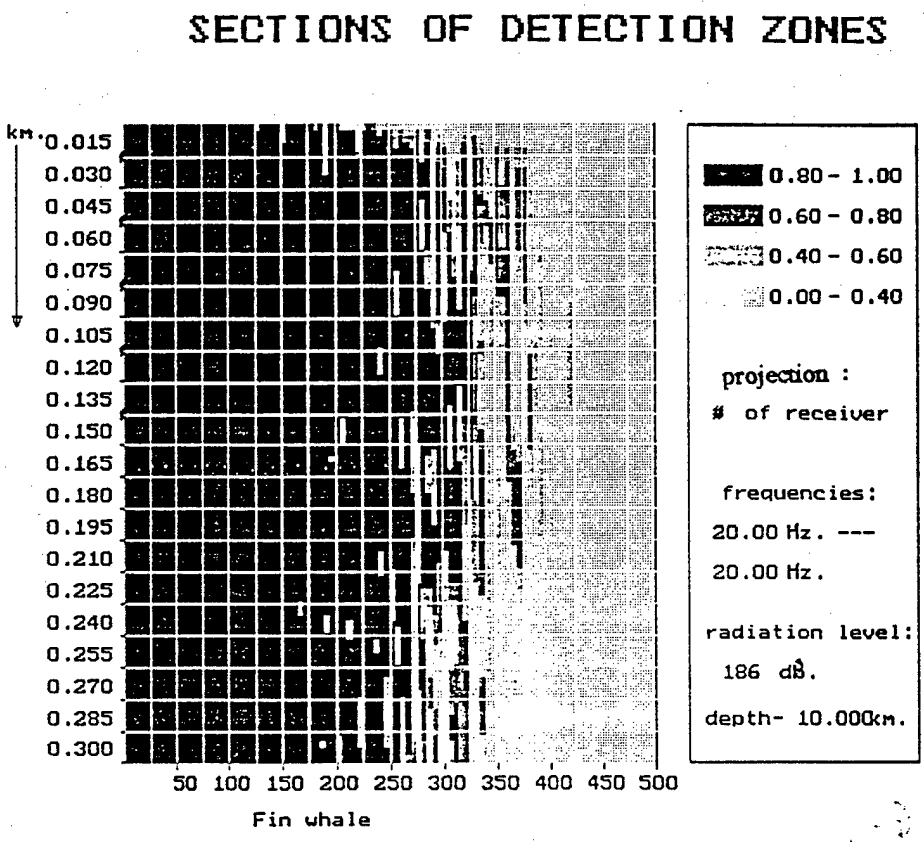

Fig. 5.2.16. Detection probability zones, vertical cross-section, a vertical array, matched processing (see legend to Fig. 5.2.9).

CONCLUSION. THE PROPOSALS ON THE FUTURE INVESTIGATIONS.

1. In this volume of the report our preliminary considerations on the principles of the SUMMM creation are presented.

2. The following results are given in brief : possible types of MM signals; possible types of radiating acoustic signals when the tags are used; description of sound propagation conditions in the given Arctic region; our approaches to sound field calculation, description of the types of ambient noise in given region.

These results have been used for the calculations of the SUMMM efficiency under various array configurations, signal-noise scenarios and so on.

These results are preliminary ones and will be improved during the progress of this project as new experimental and theoretical data will be available.

3. The variants of the SUMMM using the principles of passive location have been chosen. Such approach allows the rational compromise between the safety of MM and the SUMMM efficiency be achieved.

The two variants of the passive SUMMM based on the use of the artificial acoustic signals from tagged MM and direct signals from MM are in turn considered.

4. In typical conditions characteristic for given region the SUMMM with the use of the signals from tagged MM have operation range of the order of $1 \div 2$ km when the relatively simple processing is used.

The power source based on two nikel-cadmium cell maintains the emitter operating during one month non-stop for under pessimistic estimate taking into account the possibility of transmission of telemetric information about main physiological parameters of MM. This variant of the SUMMM is assumed to be used at first experiment for the monitoring of pinnipeds.

5. The variant of the SUMMM based on direct signals of MM is liable to give the range of the SUMMM operation up to several hundred km. The range depends on used

array, the level of MM signals, possibility of the use of information about Green function in corresponding frequency band and etc.

This type of the SUMMM is assumed to be useful in the assumed experiment in spring 1996 for the monitoring of whales.

6. The first version of program package (SUMMM-PAC) have been created as a first step to the creation of the SUMMM-PAC for analysis of the various SUMMM efficiency under different signal-noise scenarios and for the correction of the SUMMM structure under the operation of the SUMMM at the site.

The development of the first version of the SUMMM-PAC is very important problem at this stage of the project for execution of the SUMMM performance analysis.

The SUMMM-PAC is open system of programs. It allows to introduce new data about signals, statistical characteristics of noise, an array geometry, sound propagation condition in the ocean and so on together with new spatial-time processing algorithms.

The SUMMM-PAC operates in interactive regime with user. This allows to calculate the efficiency of different versions of the SUMMM for various signal-noise scenarios. Thus the SUMMM-PAC allows to design the various surveillance system for monitoring of MM in any ocean region through incorporation of corresponding data in the SUMMM-PAC.

The main purposes of the SUMMM-PAC - the design of the SUMMM, the choice of the SUMMM configuration at the site and the correction of spatial-time processing algorithms in course of service.

7. First version of the SUMMM-PAC have been used under simple models of signals, noise and sound propagation.

The ways of improvement of these models, including the perfection of spatial-time signal processing and methods of their efficiency analysis are briefly indicated. For realization of these approaches the creation of corresponding

workstation (on the base of a computer similar to "Pentium") is required in the following stage of the project.

8. Our proposals on carring out investigations aimed to the creation of first version of the SUMMM is as follows.

(i) The organization and performance (in spring 1996) of experimental investigations connected with the testing of model of the SUMMM. The main objective of the experiment is to accumulate experimental data concerning to monitoring of MM in region of ice edge in neighbourhood of Frans Josef Land, including the recording of corresponding real signals and the testing of corresponding signal processing algorithms.

(ii) The development and the creation of the following more sophisticated version of the SUMMM-PAC on the base of corresponding theoretical investigations and obtained experimental data.

9. The main theoretical investigations and corresponding computer simulation are as follows.

(i) The development of appropriate models of signals radiated both individual MM and group of the MM.

(ii) The development of effective (from computer point of view) methods of Green's function calculations for the given region of the Arctic. These programs are suggested for use both for the evaluation of efficiency of the SUMMM variants under various signal-noise scenarios and for construction of matched field processing algorithms together with their adaptive modifications. For low frequency band the use of deterministic model of Green function is appropriate whereas for middle and high frequencies the model of stochastic Green function is more reasonable.

(iii) The development and efficiency analysis of adaptive spatial-time signal processing algorithms (with adaptation to statistical characteristics both of signals and of noise) for the solution of detection, localization, and tracking problems.

(iv) The development and simulation of identification algorithms for individual MM and shoal of the MM. This is a complicated problem. Here the joint efforts both of biologist and of experts in signal processing area are required.

(v) The development of the algorithms of joint processing for global surveillance system derived from the network of the local SUMMM.

It is assumed that the details of the above will be discussed with customer, including the discussion of the organization of joint investigations.

10. Our proposals on the performance of the experiment together with American party are as follows.

(i) The creation of the model of the SUMMM with the use several vertical arrays as variant of a hydroacoustical array. The presence of a caliber sound source is implied.

(ii) The heart of this experiment is a Russian hydrographic vessel with the platform for a helicopter and a corresponding workstation on board.

This vessel is drifting in open water and in vicinity of ice's edge in the region of Frans Josef Land.

Using a helicopter stationed on the vessel board the transporting and setting on ice of the corresponding parts of SUMMM model are performed.

(iii) The experiment is performed in period of spring-summer (June, July, August) of 1996. The function of the powerful low-frequency sound source must - be provided in this period.

In great detail the plan of the experiment together with preliminary estimate of the cost is presented in the separate document.

REFERENCES

1. Low-frequency sound and marine mammals, National research council, National Academy Press, Washington D.C. 1994.

2. Milne P.H. Underwater acoustic positioning systems. 1983. E. & F.N.Spon. London, New York.

3. D.V.Sarwate, M.B.Pursley. Crosscorrelation Properties of Pseudorandom and Related Sequencies. Proceedings IEEE, Volume 68, Number 5, May 1980.

4. Zacharov Y.V., Codanev V.P. "Experimental study of acoustical communication system with the use of pseudonoise signals". Akusticheskiy Journal, 1994, v.40, N 5, 799 - 808 (in Russian), English translation "Physical Acoustics".

5. Dawson C.H. An Introduction to Random-Access Discrete Address System // IEEE Inter. Conven. Rec. 1964, pt. 6.

6. Preliminary Estimates of Low frequency Sound Effect on Sea Animals in the Eastern Arctic. A report for the Science Application International Corporation. The research group: V.M.Bel'kovich, N.G.Bibikov, N.A.Dubrovsky, M.N.Sukhoruchenko, V.A.Zhuraviev, T.V.Zorikov. Moscow, 1994.

7. Tentative Estimates of Marine Mammals Distribution and its Seasonal Variations in the Eastern Arctic. Preliminary Report for Science Applications International Corporation. Principal investigators: V.M.Bel'kovich, N.G.Bibikov, N.A.Dubrovsky. Moscow, 1995.

8. Milne A.R., Ganton J.H. Ambient noise under Arctic-Sea ice. JASA. 1964, 35, 5, 855 - 863.

9. Green C.R., Buck B.M. Arctic Ocean ambient noise. JASA. 1964, 36, 8, 1218 - 1220.

10. Ganton J.H., Milne A.R. Temperature and wind-depended ambient noise under midwinter pack ice.JASA. 1965,38, 3, 406-411.

11. Milne A.R. Statistical description of noise under shorefast sea ice in winter. JASA. 1966, 39, 6, 1174 - 1182.

12. Urick R.J.The noise of melting icebergs.JASA. 1970, 50, 337.

13. Johannessen O.M., Payne S.G., Starke e.a. " Ice eddy ambient noise "-"- . 1987, p. 599 - 606.

14. Makris N.C., Dyer J. Environmental correlates of pack ice noise. JASA. 1986, 79, 5, 1434 - 1440.

15. Pritchard R.S. Sea ice noise-generating processes. JASA. 1990, 88, 6, 2830-2842.

16. Gavrilov V.P. The ice noise in case of termic cracks in the ice. Proceeding of the Arctic and Antarctic Institute. Ice physics, 1970, v.295, 182 - 184 (in Russian).

17. Bogorodsky V.V., Gusev A.V. The ice sea noise. Review, Akusticheskiy Journal, 1968, v. XIV, N 2, 153 - 162 (in Russian), English translation "Physical Acoustical".

18. Urick R.J. Principles of underwater sound McGraw-Hill Book Company. 1975.

19. Furduev A.V. The ocean noise. In: "Acoustics of the ocean", Moscow, 1974 (in Russian).

20. J.Dyer. "The song of sea ice and other Arctic Ocean melodies" in Arctic Technology and Policy edited by J.Dyer and C.Chryssostomidis (McGraw. Hill, New-Jork. 1984), pp. 11 - 37.

21. Arctic Atlas.

22. CEAREX. Drift Group, "CEAREX Drift Experiment". EOS Transactions, Am. Geophys. Union. 71, 1115 - 1118 (1990).

23. Gavrilov A.N., Kryazhev F.I., Kudryashov V.M. The acoustic monitoring of the Arctic ocean; computer modeling. Proceeding of I session of Russian Acoustical Society, Moscow, 1993. (in Russian).

24. Gavrilov A.N., Kryazhev F.I., Kudryashov V.M. Modeling of acoustical monitoring of the Arctic ocean. Report of the Acoustics Institute, Moscow, 1993. (in Russian).

25. Gavrilov A.N., Kryazhev F.I., Kudryashov V.M. The development of methods of investigations for the analysis of the variability of Arctic climate, Report of the Acoustics Institute, Moscow, 1994. (in Russian).

26. Mikhalevsky P.N., Muench R.D., DiNapoli F.R. Acoustic measurements of Arctic ocean warming. Science Applications International Corporation Marine Technology Group. McLean, Va. 1990.

27. Aleksandrov I.A. The classification of sea ice according to the type of its underside profiles and the reflection of sound from rough ice of various types. Proc. of Russian Acad. Sci, 1994, Vol. 40, N 5, p. 738 - 742. (in Russian).

28. Voronovich A.G. Approximation of noncorrelatied reflections in the problem of sound propagation in waveguide with statistically rough boundary. Proc. of Acad. Sci. of USSR, 1987, Vol. 39, N 1, p. 19 - 30. (in Russian).

29. Kryazhev F.I., Kudryashov V.M. Sound field in a waveguide with statistically uneven admittance boundary. Proc. of Acad. Sci. of USSR, 1984, Vol. 30, N 5, p. 662 - 666. (in Russian).

30. Suzanne T. McDaniel. Physical optics theory of scattering from the ice canopy. JASA, 1987, Vol. 82. N 6, p. 2060 - 2067.

31. Lecture Notice in Physics, 70, Wave Propagation and Underwater Acoustics, ed. by Joseph B.Keller and John S.Papadakis, Springer-Verlag, Berlin, Heidelberg, New York, 1977.

32. Camp L. Underwater Acoustics. Wiley-Interscience, New York, 1970.

33. Gutkin L.S. The theory of optimal method of radio reception under noise. Moscow, 1972. (in Russian).

34. Zaharov Y.V., Kodanev V.P. "The noise stability of adaptive reception of complex acoustical signal in presence of reflection from the ocean boundaries". Akusticheskiy Journal, 1955, v. 41 (in press, in Russian), English translation "Physical Acoustics".

35. Baronkin V.M. "Statistical methods of sound field analysis in the ocean". In: "Acoustics of the ocean medium". Ed. by L.M.Brekhovskikh. Proceeding of conference on Acoustics of the Ocean, 1985. (in Russian).

36. Baronkin V.M., Dubrovsky N.A., Tarasova M.V. Information criteria for sound source location by human. Second French congress acoustic, 1992.

37. Baggeroer A.B., Kuperman A.W., Mikhalevsky P.N. An overview of matched field methods in ocean acoustics, IEEE Journal of Ocean engineering, v.18, N 4, October. 1993.